RESILIENT ENGINEERED SYSTEMS: THE DEVELOPMENT OF

AN INHERENT SYSTEM PROPERTY

A Dissertation

by

SUSAN MCALPIN MITCHELL

Submitted to the Office of Graduate Studies of
Texas A&M University
in partial fulfillment of the requirements for the degree of

DOCTOR OF PHILOSOPHY

May 2007

Major Subject: Chemical Engineering

RESILIENT ENGINEERED SYSTEMS: THE DEVELOPMENT OF

AN INHERENT SYSTEM PROPERTY

A Dissertation

by

SUSAN MCALPIN MITCHELL

Submitted to the Office of Graduate Studies of
Texas A&M University
in partial fulfillment of the requirements for the degree of

DOCTOR OF PHILOSOPHY

Approved by:

Chair of Committee,	M. Sam Mannan
Committee Members,	Ramesh Talreja
	Kenneth R. Hall
	Mahmoud El-Halwagi
Head of Department,	N. K. Anand

May 2007

Major: Chemical Engineering

ABSTRACT

Resilient Engineered Systems: The Development

of an Inherent System Property. (May 2007)

Susan McAlpin Mitchell, B.S., Texas A&M University

Chair of Advisory Committee: Dr. M. Sam Mannan

Protecting modern engineered systems has become increasingly difficult due to their complexity and the difficulty of predicting potential failures. With the added threat of terrorism, the desire to design systems resilient to potential faults has increased. The concept of a resilient system – one that can withstand unanticipated failures without disastrous consequences – provides promise for designing safer systems. Resilience has been recognized in research settings as a desired end product of specific systems, but resilience as a general, inherent, measurable property of systems had yet to be established. To achieve this goal, system resilience was related to an established concept, the resiliency of a material. System resilience was defined as the amount of energy a system can store before reaching a point of instability. The energy input into each system as well as the system's exergy were used to develop system stress and system strain variables. Process variable changes to four test systems – a steam pipe, a water pipe, a water pump, and a heat exchanger – were applied to obtain series of system stress and system strain data that were then graphed to form characteristic system response curves.

Resilience was quantified by performing power-law regression on each curve to determine the variable ranges where the regression line accurately described the data and where the data began to deviate from that power-law trend. Finally, the four test systems were analyzed in depth by combining them into an overall system using the process simulator ASPEN. The ranges predicted by the overall system data were compared to the ranges predicted for the individual equipment. Finally, future work opportunities were outlined to show potential areas for expansion of the methodology.

DEDICATION

To Mother, Daddy, Anne, and Nancy for all their love, prayers, and support. Thanks for always nurturing my creativity, challenging my assumptions, correcting my grammar, telling me to speak up, and for instilling a love for learning.

To my grandparents, Mrs. Novis Jones and the late Mr. Cecil Mitchell, for building the spiritual legacy I have been privileged to inherit. Their love, prayers, dedication, and family leadership have been an uncountable blessing, undeniable example, and undying inspiration.

ACKNOWLEDGMENTS

TABLE OF CONTENTS

LIST OF FIGURES

LIST OF TABLES

CHAPTER I
INTRODUCTION

Modern engineered systems are complex creations utilizing numerous components and interactions to accomplish a myriad of goals and create a wide variety of products. Because skills required to create these systems are increasingly demanding, system designers have become increasingly specialized. This has also resulted in an increase in the number of people involved in the design and operations process – the combined effects of these and other trends has contributed to a decrease in the ability to understand the overall operation of systems and the ability to understand all possible component interactions. These knowledge limitations coupled with systems' complexity make identifying all possible system failure modes difficult. Within chemical engineering, sophisticated tools and methods have been developed to assess the probability of failure and risk faced by certain systems, however, most of these tools rely on system designers' abilities to predict all the possible system failure modes. The added threat of terrorism has exacerbated the difficulty in protecting against and planning for unanticipated events.

Therefore, it would be desirable to design and develop systems that could withstand unanticipated faults and failures without experiencing catastrophic loss of life or property. While designing systems to withstand all possible failures may not be reasonable, it would be beneficial if failures which cannot be withstood could occur in a "graceful" manner – i.e. without sudden, unexpected breakage points and such that people could be safely evacuated.

MOTIVATION

Traditional research institutions have historically placed little emphasis on

_____

This dissertation follows the style of *Risk Analysis*.

proactive research aimed at the anticipation of unexpected failures. Response measures, including design modifications, legislative changes, and new research, have generally occurred after-the-fact. Examples of a few of these incidents include:

- New London explosion: A 1937 explosion at a Texas school led to the addition of an odorant to natural gas.[1]

- Bhopal, India chemical release: A 1984 release of methyl isocyanate killed thousands of civilians and led to the modern process safety movement through the establishment of governmental and corporate programs aimed at preventing and mitigating future chemical incidents.[2]

- September 11th attacks: The 2001 attacks on the World Trade Center and the Pentagon led to sweeping changes in airline security and governmental organization through the creation of the Department of Homeland Security.[3]

Remedial actions taken after a variety of different types of incidents show proactive research aimed at anticipating and mitigating failures could prevent some of the consequences of these failures.

One concept that shows promise in assisting with this task is resilience. Resilience can be defined semantically as "the capacity of a stressed body to recover its size especially after compressive stress.[4]" Resilience incorporates both the idea that a system or body should be strong or robust and the idea that it should exhibit flexibility or give. The strength characteristic imparts the system with the ability to withstand unanticipated failures while the flexibility aspect may allow for gradual or "graceful" failures.

RESEARCH GOALS

The goals of this research are to develop safer systems by developing the concept of system resilience by:

- Defining the term and determining how resilience is manifested in systems.
- Developing quantitative correlations such that resilience can be quantitatively assessed and compared for different systems.

- Determining how to incorporate these correlations into the design process.

BACKGROUND

While little system resilience work exists and much of the work that exists remains in the concept stage, there is a wide variety of current research aimed at developing systems with desirable concepts similar to resilience. Also, the concept of resilience has been used extensively in fields such as ecology, psychology, and materials science. Descriptions of resilience from other disciplines as well as brief descriptions of existing systems research are given below. It is hoped that by studying these examples, characteristics of system resilience can be gleaned as well as potential methods for study and assessing system resilience could be identified and leveraged for future work.

Current Definitions

The Merriam-Webster dictionary defines resilience as[4]

1) "the capability of a strained body to recover its size and shape after deformation caused especially by compressive stress"

2) "an ability to recover from or adjust easily to misfortune or change"

This definition incorporates the idea that resilience involves both the strength or robustness of a body or system as well as that system's give or flexibility.

Ecological Resilience

Ecological resilience can be defined in two different ways with one definition applying to an equilibrium view and the other to the non-equilibrium view. The two definitions are as follows:

- *Equilibrium view* – Resilience is "the ability of systems to return to their stable equilibrium point after disruption." This view assumes stable equilibrium conditions exist.[5]

- *Non-equilibrium view* – Resilience "is the ability of a system to adapt and adjust to changing internal or external processes.[5]"

The non-equilibrium definition is more general, as it can be used to describe systems with and without stable equilibrium conditions or systems with multiple equilibrium points.

Ecological resilience is generally used to describe a property or trait of an ecosystem.[6] However, what constitutes an ecosystem is somewhat arbitrary. While physical boundaries for an ecosystem can be established, external influences such as human action, policies, and institutions may or may not also be included.[5]"

Holling attempted to distinguish the between ecological definition nuances by defining them as ecological and engineering resilience. Ecological resilience emphasized the level of disturbances that the system can absorb before the system changes structure via variable or behavioral changes. Engineering resilience emphasized resistance to disturbances and how long the system requires to return to the equilibrium steady state.[7] However, both definitions were analyzed in the context of ecological systems.

While ecological resilience is generally a qualitative variable, Arrowsmith and Inbakaran developed a quantitative approach to measure the impact of tourism on ecological resilience, which they defined as "the level to which an environment, subject to some force, will respond and return to its original form.[8]" However, limitations with the study's use included that correlations were developed by first studying standardized, experimental variables and that non-parametric variables were used.[8] The resulting correlations are useful only in very narrowly defined locations and applications.

Information Network Resilience

Resilience is a term often used to describe a desired characteristic of communication, computer, and other information systems; however, the term is usually only loosely defined and is often used interchangeably with the term robustness. Resilience is usually used to describe a system's ability to continue operation when system components either fail or are attacked. However, what level of operation is required to consider the system "resilient" varies. Also, resilience is mostly used to

describe the behavior of the overall system while the resilience of individual components of the system is often not addressed.

Most research on resilient information systems focuses on the system's ability to reroute information transfer if the usual path is rendered inoperable. Thus, the end result of the information transfer is unchanged, but the system structure used to accomplish this task may be completely different. Resilient information systems often focus on the system's decision processes and procedures to combat adverse situations as opposed to the physical structure of the system.[9] Characteristics often associated with information system resilience include performance optimization, fault-tolerance, process migration,[10] error detection and concealment,[9] and network traffic management.[11]

While the widespread focus on resilience as a research topic in the area of information systems yields vast amount of useful information on properties and variables that contribute to resilience, the lack of a specific, unified definition or quantification method for resilience limits the ability to compare research results. However, tools, indices, and equations developed to measure different aspects of information system resilience are available.

Psychological Resilience

The concept of resilience is also widely used in psychology. Norman Garmezy, who studied the affect of schizophrenic parents on children,[12] first conducted academic research into the concept of resilience in the 1960's. Psychology defines resilience as "the process and outcome of successfully adapting to difficult or challenging life experiences, especially highly stressful or traumatic events.[13]" Psychological resilience not only involves resisting failure under extreme circumstances, but also positively recovering from these experiences. While individual, family, or social resilience cannot be quantified or identified by a singular set of characteristics, there are a number of factors that can contribute to resilience. These include an individual or group's world outlook and availability of resources and coping tools.

Family or group organization, stability, and connectedness tend to aid in developing resilience. Resilient individuals tend to exhibit the following traits:[13]

- Optimism
- Self-efficacy
- A sense of mastery
- A sense of coherence
- Hardiness

Maurice Vanderpol posited that resilient individuals possess a "plastic shield" which consists of factors like a sense of humor, the ability to form external attachments, and the ability to protect an inner psychological space.[12] Diane Coutu examined the issue of resilient individuals and organizations in the *Harvard Buisness Review*. She speculated resilient people have "a staunch acceptance of reality; a deep belief, often buttressed by strongly held values, that life is meaningful; and an uncanny ability to improvise.[12]" She countered the claim that resilient people are optimistic – instead, she claimed resilient people have a very grounded view of reality – they accept their situations. Applications of these ideas for resilient organizations include placing emphasis on contingency planning, establishing strong value systems, and promoting inventiveness. An organization's acceptance of current realities will allow it to objectively plan for all possible future outcomes and prevent the organization from being blinded by a false sense of security or the "that couldn't possibly happen" attitude. Establishing strong value systems or business creeds gives companies purposes beyond simply making money.[14] Value systems give employees something to work for through difficult times. Emphasizing inventiveness in an organization allows companies to survive through unpredictable circumstances. If inventiveness has been cultivated during ordinary times, it will be more likely to become habit and manifest itself during unusual circumstances.

Hamel and Valikangas further developed the idea of resilience in business by defining it as "the ability to dynamically reinvent business models and strategies as circumstances change.[14]" Instead of emphasizing recovery from crisis, they emphasized the business's ability to anticipate crises and constantly reinvent themselves. Important aspects of developing resilience in business included eliminating denial of the current state of business, valuing variety as an insurance policy against the unexpected, and

liberating resources to allow capital for innovation.[14] Dean Becker, CEO of Adaptiv Learning Systems summarized the importance of individual and organizational resilience in the following quote:

> More than education, more than experience, more than training, a person's level of resilience will determine who succeeds and fails. That's true in the cancer ward, it's true in the Olympics, and it's true in the boardroom.[12]

While lacking specific identifying factors and quantitatively measurable variables decreases the usefulness of psychological resilience in scientific research, studying how people adapt could help identify corresponding, measurable variables in systems.

Materials Science

Materials science defines resilience as "the ability of a material to absorb energy when deformed elastically and to return it when unloaded[15]" or the "extent to which energy may be stored in [a material] by elastic deformation.[16]" Material resilience is usually measured in terms of the modulus of resilience, which is the area under the stress-strain curve (Figure 1) from zero stress to the yield stress, or the "strain energy per unit volume required to stress the material from zero stress to the yield stress σ.[15]"
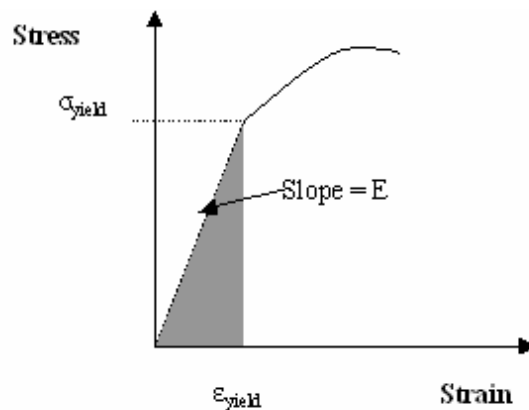
Figure 1: Linearly Elastic Stress-Strain Diagram

For a linearly elastic material, the modulus can be expressed as[15]

$$U_R = \frac{1}{2}\frac{\sigma_{yield}^2}{E}$$
(1.1)

where

σ_{yield} = elastic limit

E = modulus of elasticity

Resilient materials generally have a high yield stress and low Young's modulus. Examples of materials with high moduli of resilience include rubber and high-carbon steel springs. Because rubber and some other synthetic polymers have high moduli of resilience, materials consisting of these materials are sometimes also called resilient. For example, resilient floor coverings are defined as "floor coverings based on synthetic thermoplastic polymers.[17]" Resilient wheels are wheels where a rubber layer has been included between the tread and web.[18]

Material resilience can be assessed and compared for a wide variety of materials. Material resilience is generally measured using a uniaxial stress and thus resilience can vary depending on the direction of stress for anisotrophic materials. This is not a concern for isotropic materials since material properties are not affected by direction in these materials. Also, for non-linearly elastic materials, the earlier modulus of resilience equation given is not applicable and integration techniques must be employed to quantify resilience by computing the area underneath the stress-strain curve.[19]

Related Research

The term resilience is often used in a variety of research settings to describe related characteristics and properties. While not all of these may apply to all systems, it is helpful to study these in order to determine how researchers envision resilient systems behaving.

Self-Healing

Resilient systems are often described as self-healing. Self-healing is an attractive property because it reduces the system's need for error/fault management and reduces the amount of outside or human intervention and maintenance required for normal system operation. The degree of self-healing exhibited by system varies.

When materials are described as self-healing, they generally do not require any type of outside intervention and often have inherent fault or crack detection mechanisms. One example of a self-healing material is the self-healing plastic developed by White et al.[20] The plastic contains embedded catalyst and polymer pellets that release polymer via capillary action when a pellet is intercepted by a crack. The polymer then reacts with the catalyst to form new plastic to fill the crack. The healed plastic has been shown to recover 75% percent of its pre-cracked toughness. The main benefit of this material is that human intervention is not required to begin the healing process, however drawbacks include the limited nature of the healing mechanism (once the pellets are used up, the healing cannot occur) and the fact that the plastic is still in the developmental stage for high-load applications.[20]

Another example of a self-healing plastic is thermally cross-linked polymers.[21] These polymers are highly cross-linked polymers that can heal cracks by exposing the plastic to higher temperatures that allows bonds to reform across cracks. One example, a polymer formed by a thermally reversible Diels-Alder reaction, has been shown to recover about 57% of its original fracture load. These plastics can crack and re-heal many times under mild conditions, however varying temperature or intervention is required to begin the healing process.[21]

Princeton researchers have developed a self-healing material using electrohydrodynamics.[22] The research used two concentric cylinders with the annulus filled with a colloidal dispersion of polystyrene particles. An electric current applied across the cylinders allowed the current density to change at the sites of defects. This allowed particles to coagulate at the defect site. Healing occurred when salts in the colloidal dispersion electrochemically deposited in the void spaces between the

coagulating polystyrene particles.[22] These examples of self-healing materials are attractive because they repair damage while it is still at the micro-level – ideally damage is reversed before it can become a serious problem.

Nanoparticles have also been used in the development of self-healing composite materials.[23] University of Pittsburgh researchers added nanoparticles to polymers to allow the nanoparticles to repair damaged areas of the polymer. The added nanoparticles were the same substance as the original material thus allowed the healed material to have similar material properties as the pre-damaged material. It was assumed that the particles "patched" damaged areas of the polymer faster than damage spread thus forming a crack extension barrier.[23]

Computer systems can also be described as self-healing. Self-healing computer systems generally are programmed to have a specific self-healing mechanism. Koopman summarized the self-healing computer system problem into four divisions – fault model, system response, system completeness, and design context.[24] The fault model involved the system's ability to detect errors and the system response involved how the system reacted to the faults. System completeness addressed limitations in the system's knowledge and how this affected the system's healing power while the design context dictated how self-healing abilities affected the system's normal operation.[24] Each of the four categories contained numerous model elements, which are shown in Table 1.[24] These could potentially provide parallels for important properties within other systems.

Table 1: Elements of a Self-Healing Computer System

Model Element	Fault Model	System Response	System Completeness	Design Context
Model Element Properties	Fault duration	Fault detection	Architectural Completeness	Abstraction level
	Fault manifestation	Degradation	Designer knowledge	Component homogeneity
	Fault source	Fault response	System self-knowledge	Behavioral predetermination
	Granularity	Fault recovery		User involvement in healing
	Fault profile expectations	Time constants	System evolution	System linearity
		Assurance		System scope

Another example of a self-healing system is living organisms. Biological systems are the most sophisticated examples of self-healing systems that currently exist. The human body can repair a multitude of faults including attack by bacteria and other viruses, repair of the skin from cuts and other contusions, and healing and/or re-growth of bones and other damaged cells.[25]

Self-Managing

Resilient computer systems are sometimes described as being self-managing or self-configuring. Generally, this refers to the system's ability to change its organizational structure to adapt to specific scenarios. For example, if part of the computer network was under attack from a computer virus, a self-managing system could transfer important tasks from the attacked part of the network in order to allow the network to continue operation.[26] Self-configuring (or reconfiguring) networks also must also be able to reroute information through alternative paths if information transfer paths are damaged or otherwise rendered inoperable.

Much of the reconfiguring behavior of systems draws inspiration from natural structures. Animal organizational structures are highly reconfigurable – for example,

within ant colonies, tasks such as food gathering, threat alerting, and home building can be redistributed depending on available personnel.[26]

Redundant

System redundancy involves having multiple components within a system that can perform the same function. Redundancy can manifest itself in multiple ways – there can be multiple identical components within the system that perform identical functions in order to check each other, there can be back-up components in the system that only operate if the primary component fails, or there can be different components that can perform the function of other components under extreme circumstances. One example of the multiple operating components within a system is sensors within a control system. Often, for crucial measurements, three operating sensors are installed with the value taken as the consensus of the three – for example, if one fails, its value is essentially out-voted by the other two. This eliminates the possibility of control system malfunctions due to random failures of individual sensors. An example of a back-up redundancy is spare electric generators. These generators are employed at critical locations such as hospitals where power failures could be catastrophic. If the primary power supply fails, the back-up generator begins operation, allowing continual supply of power.

Biological systems exhibit high levels of redundancy. Millions of cells performing identical functions exist. Cells are produced and die continually – numerous cells repeat functions so that the loss of individual cells makes little difference.[25]

Scalable

Another characteristic of some resilient systems is scalability or the system's ability to add or decrease capacity. This characteristic emphasizes the system's ability to handle differing levels of network traffic or changes in the system's physical structure. It is important for the systems to seamlessly scale without affecting ongoing system operations.[26] The idea of a system having spare capacity is often coupled with its

reconfigurability, as a system with spare capacity can allow demand to be easily rerouted throughout the system.[27]

Decentralized

A term often used with electric power grids or information networks is decentralized. Decentralized, or distributed, systems spread tasks over a wide range of different components. This prevents the entire system structure from being affected in the case of a localized failure/attack/catastrophe.

Robust

Robust is defined by the Merriam-Webster dictionary as:[28]

1) "having or exhibiting strength or vigorous health"

2) "having or showing vigor, strength, or firmness"

3) "strongly formed or constructed: sturdy"

Robustness and resilience are often used interchangeably, however, robustness emphasizes strength and sturdy construction while resilience emphasizes elasticity or ability to give/deform and return to pre-stressed shape.

Robustness was defined by Carlson and Doyle in reference to complex systems as "the maintenance of some desired system characteristic despite fluctuations in the behavior of its component parts or its environment.[29]" Again, this emphasizes the systems ability to resist failure, but does not place as much weight on recovery abilities.

Specific System Examples

There are a few examples of specific systems that have been researched from a resilient perspective. Within chemical engineering, the main example is that of a resilient control system, however examples from other disciplines include power grids and naval ships. Systems for power plants have been developed which can anticipate changes in electricity demanded and thus ramp up or scale back electrical production in response.

These systems can also assist with electricity distribution by supplementing the grid with generators when demand increases.[30]

Naval ships have been engineered which can reroute operations around damaged areas of ships in order to allow the ship to reach port or continue fighting in case of an attack situation. Modular designs allow other sections of the ship to take over functions and power from the damaged areas.[31]

Researched by Morari[32] in the early 1980s, resilient control systems tolerate fluctuations by their system structure, control structure, design parameters, and control parameters.[33] The control system's resilience is limited by any non-minimum phase elements such as right-half plane zeros, physical constraints on manipulated variables, and plant/model mismatch.[33]

Morari developed a set of synthesis rules to assist the development of resilient control systems. These included:[32]

- "Choose systems where the manipulated variable has a large effect on the controlled output."
- "Choose systems where the manipulated variable is 'close' to the controlled variable."
- "Avoid systems with inverse response characteristics."
- "Avoid systems with varying parameters and strong nonlinearities."

These control systems have generally been applied for distillation columns and heat exchangers, however, the tools developed for these systems may provide insight for general system assessment.

SUMMARY

This research seeks to establish the concept of resiliency as a systems property such that safer, more secure engineered systems can be designed and operated in a manner that addresses current challenges. The introduction, motivation, and goals for this research have been presented as well as background research related to future project direction and development.

CHAPTER II
FRAMEWORK OF EXISTING RESILIENCE RESEARCH

After studying the background of resilient research and examining some of the past applications of this concept, it became clear that the scope of this research and a specific definition of system resilience would need to be established before the concept could be further developed.

RELATION TO OTHER RESILIENCE RESEARCH

Since engineered and social systems are complex, the need for interdisciplinary research to more fully understand their behavior has become imperative. As partially described in the previous chapter, resiliency has been widely used to describe a desired trait of complex systems such as computer networks, electrical power grids, financial markets, or social systems, so before a definition is even established, it is important to determine how this research fits into the overall resilience picture.

The behavior and operation of modern systems is generally not completely understood because of their complex structure, diversity of system elements, and difficulty of defining system boundaries, among other factors. Improving the understanding of the behavior and operation of these systems requires input from a variety of disciplines. For example, to properly understand the operation of the electric power grid, a researcher must have input from a variety of experts including electrical engineers, computer scientists, control engineers, grid operators, and economists. Thus, while this research focuses on assessing the physical properties of engineered systems, it only provides limited assistance with aspects related to human decisions associated with the system, informational flows affecting the system, or economic factors which impact the system.

Some of the previously given examples of resilient research (psychological resilience, ecological resilience, etc) are applicable to non-physical system aspects, thus the boundaries and scope of the studied system should be clearly defined to avoid

duplication or conflict of application.[34] Is the system strictly physical or are associated information flows and human effects included? Some possible ways of classifying systems are listed below.

- *Physical* – Physical systems consist of materials or equipment. Physical systems and system components can be defined by physical dimensions and are subject to measurable material stresses. Examples of physical systems include a material and its associated stresses, a piece of process equipment such as a pump or heat exchanger and its associate material flows and stresses, or a material flow itself and its associated stresses. Physical system boundaries can be defined by enclosing the system with boundaries and including any energy and material flows across those boundaries.

- *Informational* – Informational systems include knowledge and information flows. Information sent over network connections and commands sent to different process controllers are examples of information systems. Information systems can experience perturbations without experiencing any type of physical error or failure. Perturbations in information systems generally involve either changes in the information's integrity or failure of the system's ability to transfer the information.

- *Financial / Economic* – Financial or economic systems involve money and monetary assets. Economic systems are generally intimately integrated with information systems, as information exchange often leads to money transfer. Economic system perturbations can be measured in terms of dollars or other desired monetary units. Economic systems offer a promising unifying ability because many aspects of physical and informational systems can be described in terms of monetary terms such as cost, profit, or loss.

- *Human / Behavioral / Social / Organizational* – Behavior or social systems are systems that involve humans and their interactions. Behavioral systems are among the hardest to study and predict since human behavior and interaction are not governed by any immutable laws or rules. Social groups and organizational

structures are examples of behavioral systems since they primarily consist of humans and their relation to each other. Perturbations in behavior systems can be extreme situations, catastrophic events, or other identifiable personal stress.

SYSTEMS APPROACH AND SUSTAINABILITY

One approach to dealing with the multi-faceted resilience challenge is to use a systems approach that incorporates system impacts from a variety of disciplines.[34] One example of a current method of this type is industrial ecology, where the modeling of industrial systems is shifted from a linear model to a model with cyclic flows similar to natural systems.[34] The goal of this approach is to minimize waste, since in nature, the waste of one organism or system provides fuel or nutrients for another connected organism. Another example, thermodynamic life cycle analysis (LCA), has been applied at Ohio State University by "modeling an industrial system as a network of energy flows governed by the laws of thermodynamics.[35]" This analysis takes an "input-side" approach where resource consumption is determined in terms of exergy, or available energy. Modeling of complex decision-making strategies has also been studied to better understand adaptive system management rather than point optimization. Yet another related approach is biocomplexity, which seeks to understand the connections between human and biophysical systems. This interdisciplinary research focuses on better understanding the "complexity, dynamics, and nonlinear nature of these interdependent systems.[35]"

Since these methods have strong ties to the natural or biological world, it is understandable that one goal of this work is to improve global sustainability. However, as the complexity and interdependency of systems is better understood, it becomes clearer that any type of perturbation or shift in system structure will cause material and energy flow changes and disruption, thus the importance of a system being resilient, adaptable, and survivable to these changes become more important.[35] The EPA has even come to recognize the importance of resilience in addressing the sustainability challenge, as evidenced by this list of important challenges to sustainability:[35]

- "Addressing multiple scales over time and space."
- "Capturing system dynamics and points of leverage or control."
- "Representing an appropriate level of complexity."
- "Managing variability and uncertainty."
- "Capturing stakeholder perspectives in various domains."
- "Understanding system resilience relative to foreseen and unforeseen stressors.

While this research will not directly address sustainability, these goals make it clear that understanding resilience in general will assist with ongoing sustainability work.

RESILIENCE DEFINTION

Since the resilience challenge incorporates a variety of disciplines and system types, establishing a generally applicable definition is important. Fiksel[35] has voiced a general definition applicable to all systems:

> *Resiliency is the "capacity of a system to tolerate disturbances while retaining its structure and function."*

For each different type of system, the disturbance, or perturbation, the system withstands can be defined differently. Withstanding the perturbation involves both resisting damage or failure during the perturbed time period and returning to normal operation after the perturbation is removed. Some possible examples of different types of research, systems, and perturbations are listed as follows in Table 2:

Table 2: Perturbation Types

Research Topic	System	Perturbation
Materials Science	Physical	Energy / Applied Stress
Ecology / Drought Mitigation	Physical	Rainfall
Communication Systems	Information	Data Corruption
Accounting / Capitalism	Economic / Financial	Money / Capital
Psychology	Behavioral/Social	Personal Stress / Change in Routine

However, even if resilience could be easily assessed, measured, and analyzed for each of these system types, most systems do not fit into only one of the above categories. Most systems of interest incorporate components, aspects, and influences from multiple system types. For example, a computer network has physical, informational, financial, social, and human aspects. Each system is therefore affected by multiple perturbations. The challenge is then to determine overall system resiliency when the resiliency is affected by a wide variety of factors and variables.

In order to approach this problem, the researched system can be studied via a systems approach or it can be divided into subsystems each representing aspects such as physical, informational, financial components of the overall system. While the systems approach will generally give a more accurate overall picture, either of these approaches will allow the system to be affected by multiple perturbations.

RESEARCH SCOPE

This research will solely focus on the resilience of physical systems. No human decisions, economic factors, or organizational issues will be included. Studied systems will include material flows and equipment. While the determination of overall system resilience is an important challenge, this research will only focus on defining, analyzing, and assessing physical resilience. Also, while future applications of this work may involve sustainability aspects or approaches, this research will not directly study or address sustainability.

This research will assist with the first, third, and last of the previously state EPA objectives. System dynamics will be studied by determining how systems behave under different disturbances or perturbations. Since disturbances will be applied, variability will be introduced into each system. While this research will be limited to foreseen or applied stressors, it is hoped that studying the affects of applied disturbances will yield information useful to the understanding and protection of systems from the affects of unknown disturbances or stressors.

PHYSICAL SYSTEM RESILIENCE

When developing the physical system resilience concept, it was important to keep in mind that the definition should be general enough to allow it to be applied for a wide variety of system types. While the concept will initially be tested using chemical process systems, ideally the definition and subsequent framework would be applicable to engineered systems from other disciplines.

Along with the definitions mentioned earlier from ecology, psychology, information systems, and materials science, Kletz[36] defines resilient operation of nuclear plants as operation such that "safety systems do not interfere with the operation and maintenance of the plant, and thus there is no incentive to by-pass them." Morari[32] defines a resilient control system process as "sufficiently flexible, operable, and controllable" allowing the plant "to move fast and smoothly from one operating condition to another and to deal effectively with disturbances."

However, the drawback of these definitions is that they do not directly address the idea that resilience should be an inherent property of systems in a way that it can be assessed and measured quantitatively such that comparisons between systems are possible. The ecology and psychology definitions touch on the idea of resilience as an inherent property, but neither of these applications includes a straightforward and universally applicable method for quantification. However, the materials science application does apply resilience as an inherent, quantifiable property. Therefore, the material resilience definition will be consulted for inspiration for defining system resilience. The resilience of a material can be defined as the amount of energy the material can store without permanent deformation. Similarly, system resilience will be defined as the amount of energy a system can store without failure or instability.[19] The use of energy is desirable due to energy being a concept applicable to a wide variety of systems and disciplines.

SUMMARY

A definition has been stated to allow the physical resilience concept for engineered systems to be developed. The scope of this research has also been established and a general framework for viewing the resilience of complex systems has been briefly outlined with the goal of clarifying this research's relation to other definitions of resilience and research efforts.

CHAPTER III
CONCEPT DEVELOPMENT

Now that a definition for physical resilience has been defined and how this research relates to similar work has been explored, the concept must be developed and variables, correlations and methods must be established to allow resilience to be analyzed. Since resilience has been defined in terms of energy, concepts related to system thermodynamics may yield variables or concepts useful for the resilience concept.

IRREVERSIBILITY AND EXERGY

Material resilience is by definition cyclic (the absorption and subsequent release of energy), however, this aspect of the concept cannot be directly applied to systems since by the second law of thermodynamics real systems are irreversible. While system resilience cannot be viewed as the region where the system operates in a reversible manner, the sources of irreversibility may yield useful information about how the behavior of the system changes for different energy levels applied to the system.

While energy cannot be destroyed, it can be dissipated such that the process cannot be reversed without adding additional energy. Examples of sources of irreversibility within physical systems include:[37]

- Unrestrained expansion
- Spontaneous chemical reaction
- Heat transfer across a finite temperature difference
- Current flow through resistance
- Mixing
- Friction

Using a system energy balance will yield an incomplete picture of the system's behavior due to the fact that sources of irreversibility do not destroy energy. Also, the amount of energy within a system is not necessarily representative of the usefulness of the energy.

For example, a small bottle of water at room temperature and pressure contains a measurable amount of internal energy in the water. However, this water has little potential to perform work on its surroundings, so there is little concern about the danger of this energy. The concept of exergy offers the ability to capture in one balance equation information concerning the system's energy and entropy performance as well as that energy's potential.

Exergy can be seen as being a measure of the "usefulness" of energy.[38] This can be illustrated by considering an isolated, perfectly insulated fuel source. If the fuel is burned in air, then the final products will be warm smoke and other combustion products. This can be seen in the pictures in Figure 2.[39]

Figure 2: Exergy Destruction in an Adiabatic Process

If we assume these systems are isolated and adiabatic (perfectly insulated), they contain the same amount of energy. However, the first system has the potential to do work on another system if the user so desired – for example, the fuel can be burned to power machinery. It can drive other energy processes or be converted to another type of energy. The last system can do minimal work – while there is energy contained in the waste products, it is challenging to extract this energy. While energy has been conserved in this process, exergy has not been conserved. Exergy is defined by Szargut as:

> Exergy is the amount of work obtainable when some matter is brought to a state of thermodynamic equilibrium with the common components of the natural surroundings by means of reversible processes, involving interaction only with the abovementioned components of nature.[38]

In order to quantify exergy, a reference or dead state that corresponds to the state of thermodynamic equilibrium with the natural surroundings must be defined. For temperature and pressure, the dead state can be defined as the state of the atmosphere (generally taken as 70°F and one atmosphere of pressure). Determining reference exergy states for chemical composition or potential is more difficult and can vary slightly depending on the application, however it can be generally defined as the concentration or chemical potential of the element in the atmosphere for a vapor state, in sea water for liquids, and in the earth's crust for solids.[40] Exergy has the same units as energy, which allows for the formation of dimensionless ratios.

A general equation for exergy is shown below:[41]

$$Exergy = U + P_0V - T_0S - \sum_i \mu_{i,0} N_i \tag{3.1}$$

Where:

U	=	system internal energy
P_0	=	reference state pressure (1 atm)
V	=	system volume
T_0	=	reference state temperature (70°F)
S	=	system entropy
$\mu_{i,0}$	=	reference chemical potential of component i
N_i	=	number of moles of component i

It can be seen that exergy is based on and calculated from basic thermodynamic principles. For certain special cases, exergy differences can be simplified to more familiar thermodynamic functions. For a process that occurs at the reference temperature that does not involve a change in volume or the number of moles, the change in exergy is the change in the Helmholtz free energy. For a process occurring at the reference pressure without changes in entropy or the number of moles, the change in exergy can be

calculated as the change in enthalpy. For a process at the reference temperature and reference pressure involving no change in moles, the change in exergy is simply the change in the Gibbs free energy.

Exergy can be classified into different types including kinetic, chemical, mixing, and potential exergy. The exergy of a process stream can be classified as follows:[38]

$$B = B_k + B_p + B_{ph} + B_{ch}$$
(3.2)

Where:

B = stream exergy

B_k = kinetic exergy, where kinetic exergy is equal to the kinetic energy when the reference state is assumed to be the velocity of the earth

B_p = potential exergy, where potential exergy is equal to potential energy when process is operated as sea level

B_{ph} = physical exergy

B_{ch} = chemical exergy, where chemical exergy is due to the difference between atmospheric and system chemical composition

Most chemical operations do not involve significant changes in the overall elevation or velocity of the process. While the actual component stream may change elevation or velocity, the process itself does not. Therefore, the kinetic and potential terms will be neglected and only the thermal exergy calculated. Thermal exergy is:

$$B_{th} = B_{ph} + B_{ch}$$
(3.3)

Where:

B_{th} = thermal exergy

Many chemical operations are flow processes. For a flow process which does not involve mixing or chemical reaction, the chemical exergy term will not appear and thus the exergy of a flowing process stream can be calculated as the physical exergy using the following equation.[40]

$$B_{ph} = H - H_0 - T_0(S - S_0)$$
(3.4)

Where:

H =   enthalpy of stream at process T and P

H_0 =   enthalpy of stream at T_0 and P_0

ENERGY AND SAFETY

While analysis of a system's energy, exergy, and irreversibilities provide useful information about the system; the question of what they have to do with safety must be answered. Since the concept of resilience is being developed with the idea that it could be used to develop safer systems, some safety justification must support the use of these values in concept development.

Many safety incidents can be classified as "loss of containment" events. Loss of containment means that the process materials or fluids somehow escape their normal boundaries. One example of this includes over-pressuring a vessel such that the safety relief device opens releasing liquid or vapors into the atmosphere or into a flare header. Another example could be a pipe that is struck such that a hole forms resulting in process fluid leaking. While different failures occurred to result in these loss of containment events, in both events the system could not withstand the amount of energy applied. All systems are designed to withstand some range of applied energy amounts, or energy loads. If a load outside that range is applied, then the system may experience a failure since it was not designed to operate under those conditions. Therefore, more accurately studying both what range the system can tolerate and the behavior of the system at different energy loads could help determine more precisely where the system can safely be operated.

The resilience concept can aid in the determination of appropriate operating ranges if systems are assumed to be designed to operate safely at their initial conditions. Then, the study of how the system's behavior changes for different energy levels will yield information on when the system either behaves in a manner similar to the initial behavior (for example, temperature gradually increasing in a reactor as the coolant temperature is increased), or if behavior begins to shift to unpredictable or unexpected

types (for example, temperature rapidly increasing after coolant temperature is raised above a certain threshold).

CORRELATION DEVELOPMENT AND VISUALIZATION

Since material resilience is being used as a conceptual analogy to develop and motivate the system resilience application, material resilience will be studied to aid in determining how to further frame the system resilience definition and quantification efforts. Just as material resilience can be used as a selection criterion to identify appropriate materials for a specific application, the goal is that the conception of system resilience can be developed to yield a similarly useful selection criterion to identify appropriate system designs for maximizing the system's ability to survive and operate under a variety of conditions. Material resilience allows the user to determine appropriate ranges -- both how large of an energy load can be applied without permanent damage and how far the system can deform without permanent damage. System resilience may yield similar useful ranges that can be used to determine under what conditions a system can be safely operated.

Since physical systems are composed of many different materials, the behavior of these systems may in some way resemble their material components. Material resilience incorporates multiple aspects of physical behavior – it includes the impact of the material's stiffness in assessing how much force or stress the system can withstand in a reversible manner as well as the material's flexibility to determine to what degree the system can reversibly deform to allow greater energy storage while still remaining in the reversible, elastic behavior region.

Material resilience can be easily visualized and quantified using a stress-strain diagram - the stress-strain curve can be used to identify where the system's behavior or response to an applied force changes from a reversible elastic behavior region to an irreversible plastic region. In the elastic region, the applied force results in energy storage within the material by reversibly deforming while in the plastic region the additional applied force is dissipated by permanent material deformation. Even though

permanent deformation occurs, the permanent deformation protects the material from permanent fracture or failure. In a linearly elastic material, the transition from elastic to plastic deformation occurs when the stress-strain curve transitions from a linear relationship between stress and strain to a non-linear relationship. However, not all materials display a linear slope in the elastic regime.

It would be desirable to develop a similar diagram for systems that could summarize the system's behavior. It may be possible to create a stress-strain system curve that could be used to identify a resilient behavior region wherein the system displays a specific type of behavior or graph shape in response to applied forces. These graphs could be used to identify when the system behavior changes or departs from the resilient behavior regime, thus identifying ranges where the system behaves in a predictable manner. While a transition from a linear graph shape to a non-linear curve may characterize the resilient to non-resilient transition for systems, like materials, the resilient regime may not display a linear trend for all systems.

If such a graph is created, a definition for system stress and a definition for system strain must be established. The terms from materials science will again be consulted for inspiration.

Stress

Stress is a measure of the applied load to a system or body while strain is a measure of a system's response (generally in terms of a deformation) to that applied load. Physically, stress is also a measure of a body's internal force distribution.[42] Material stress is measured in dimensions of force per unit area and measures the load on a material per unit area.

The "load" applied to a system could be viewed as the amount of energy contained within the system. Measurements of stress require the applied "load" to be normalized by dividing it by the dimensions the "load" is acting on. For systems, the "load" is acting over three dimensions; therefore the energy of the system will be taken as acting over the system's volume. Thus, the system stress (Ss) will be represented as:

$$Ss = E_{in} / V_{sys} \tag{3.5}$$

Where:

Ss = system stress

E_{in} = input energy into system

V_{sys} = system volume

One significant difference between the material stress variable and defined system stress variable is the units – while the material stress variable has units of force per unit area, the system stress variable has units of energy per unit volume per unit time. While force per unit area is dimensionally equivalent to energy per unit volume, the presence of the additional time variable is different. The time variable is due to the presence of energy flows within systems – its presence also yields information about how the rate of the process affects the system's behavior. While the time variable could have been eliminated had the energy rate been divided by the volumetric flow rate into the system, this would not have captured information about how the dimensions of the system affect its behavior. Also, this would have made assessing changes in system behavior difficult for changing mass flow rate cases – for example, if only the mass flow rate is changing and the system only has material stream inputs, the system stress variable would not change if the mass flow rate into the system were doubled due to the fact that both the energy into the system and volumetric flow rate into the system would double.

The use of energy to characterize system stress is particularly useful due to the near-universal presence of energy measures for different system types. Using general scientific principles such as input energy will allow the system resilience methodology to be applied to systems from a variety of different discipline without concern over the translation of discipline-specific variables.

Strain

Material strain is non-dimensional and measures elongation per unit length. For measurement of material strain, the material is generally being stressed by applying a force along one axis of the material. The applied force causes the material to eventually

deform by lengthening along the axis the force is being applied. Thus, the elongation is a straightforward variable that can be easily measured to assess the system's degree of deformation.

Systems do not have an equivalent straightforward variable that can assess how the system "deforms" for different applied stress – systems deform in a variety of ways. Since many variables are involved in determining how a system deforms, the original cause of that deformation or strain will need to be explored. The applied energy load causes the strain, but all the energy applied to the system does not have the potential to deform it. Only the portion of the applied energy that has the potential to do work on either the system or its surroundings can cause strain. Exergy is a measure of this energy potential, so system strain will thus be defined as a ratio of the system's exergy. Since system strain should also be non-dimensional and measure some normalized response of the system, the deformation of the system will be viewed as the exergy destroyed by the system (equivalent to the exergy into the system minus the exergy out of the system). Thus, system strain (Sn) will be initially defined as the exergy destroyed by the system over the initial exergy input into the system.

$$Sn = Ex_{destroyed} \ / \ Ex_{in} \tag{3.6}$$

Where:

$Ex_{out} = Ex_{in} - Ex_{destroyed}$

Ex_{in} = exergy inputed into the system

$Ex_{destroyed}$ = exergy destroyed within the system

Again, the use of principles derived from fundamental thermodynamics allows the development of a general methodology that could potentially be applied to systems from a variety of disciplines.

System Stress-Strain Curve

These variables of system stress and system strain can be used to create a characteristic system response curve that can be thought of as the equivalent stress-strain curve for a system. These variables will be tested to ensure they appropriately capture

system behavior by developing various simplified test systems from process engineering. Changes in the stresses applied to each system will be accomplished by incremental variable changes.

Variable Behavior

Examining the behavior and ranges of the proposed variables yields important information. The proposed stress variable can range from zero to higher values – the only limit is the energy and volume of the system, with the zero stress point indicating there is no energy present in the system. The proposed strain variable can range between zero and one, with the point of zero strain indicating no exergy is destroyed by the system while the point where the system strain equals one indicating the system destroys all the exergy initially present within the system.

However, unlike the analogous material stress strain curve, the characteristic system curve does not begin at the point of zero stress and zero strain. The point of zero stress and zero strain is impossible – the zero stress point would require the absence of all energy, even internal energy. Because of the presence of zero point energy, this could not be achieved even at absolute zero.[43] The zero strain point is not achievable due to the fact that it would require the process's change in entropy to equal zero, which is only achievable in hypothetical perfectly ideal processes or at absolute zero.[44]

Thus, the characteristic system curve will begin some point above zero stress and strain and could potentially range as high as strain equals one. However, the point of strain equals one is also not likely, since this would indicate the process was destroying all potential to do work on its surroundings. Processes destroying all exergy would require the material streams to be at the temperature and pressure of the surroundings at exit. So, while the point of zero strain indicates a perfectly ideal process and the point of strain equals one indicates a perfectly inefficient process, neither is likely.

Because the curve does not begin at zero stress and strain, the stress and strain can either increase or decrease as it moves away from the initial point and the variables can either be directly or indirectly related. For example, if the strain increases as the

stress on the system decreases, this indicates the system operates more efficiently at higher stress values. If the stress and strain both increase, the system's efficiency is decreasing as the stress applied to the system increases.

While a strain value close to zero indicates the system is operating efficiently, low strain values do not necessarily indicate whether or not the system is operating safely: that depends in part on how the system is designed to operate. While the values of the stress and strain variables are of use to compare the magnitude of systems, how the variables change with respect to system fluctuations is of primary interest. Systems will be assumed to have been designed to operate safely and satisfactorily under initial conditions – while systems have been known to fail under normal conditions, most unexpected failures occur during upset conditions as the system responds to abnormal situations in an unexpected manner. Thus, determining whether or not systems respond to changes in expected ways is important in determining whether or not a system can continue to be safely operated under a certain range of conditions.

SUMMARY

The concept of system resilience was further explored by determining that it would be desirable to have a representative system curve to allow system resilience to be displayed, compared, and qualitatively assessed. Variables of system stress and system strain were defined to allow such a curve to be created.

CHAPTER IV
TEST SYSTEMS

To further develop the concept of system resilience and to obtain preliminary results for the qualitative assessment of system resilience, simple test systems from process engineering were developed. The systems studied include a steam pipe, a water pipe, a water pump, and a heat exchanger. Properties as well as applicable assumptions and calculations are explained for each system.

SYSTEM PROPERTIES
Steam Pipe

Since simplicity was desired for preliminary testing of the resilience concept, the first test system chosen was a steam pipe. A steam pipe was desirable since it contains only one material component whose properties can be determined for a wide range of conditions using steam tables. The pipe was assumed to not have fittings or insulation. The pipe roughness was taken to be light rust on carbon steel. The steam was assumed to be superheated to allow temperature and pressure to be changed independently. Properties such as roughness and heat transfer properties were assumed to be uniform along the length of the pipe. The pipe was assumed to be a carbon steel schedule 40 pipe with standard wall thickness. While temperature stresses would be present when the pipe was heated about certain levels, this affect was not included due to its complexity. Properties of the system are listed below in Table 3.

Table 3: Pipe Test System Properties

System Property	Value	Units
Pipe length, $L =$	50	Ft
Reference state temperature, $T_0 =$	70	^oF
Nominal inside diameter, $D_{nom} =$	5	in
Pipe roughness, $\varepsilon =$	0.04	in
Heat transfer coefficient of air, $h_{inf} =$	18	Btu/hr-^oF

Water Pipe

Along with the steam pipe, a water pipe was studied. The water pipe was assumed to have the same physical properties (diameter, length, roughness, etcetera) as the steam pipe with the exception that water was chosen as the pipe's single component. The water was assumed to be subcooled to allow temperature and pressure to be changed independently.

Water Pump

The resilience concept was also applied to an adiabatic centrifugal pump water pump. The pump test system allowed for more complexity due to the fact that all variables cannot be changed independently. For example, the volumetric flow rate through the pump is related to the pump head as shown by the pump curve below in Figure 3. This curve was used to determine how the pump head and efficiency change as the volumetric flow rate changed. The pump curve below uses data taken from *Centrifugal and Rotary Pumps – Fundamentals With Applications.*[45]
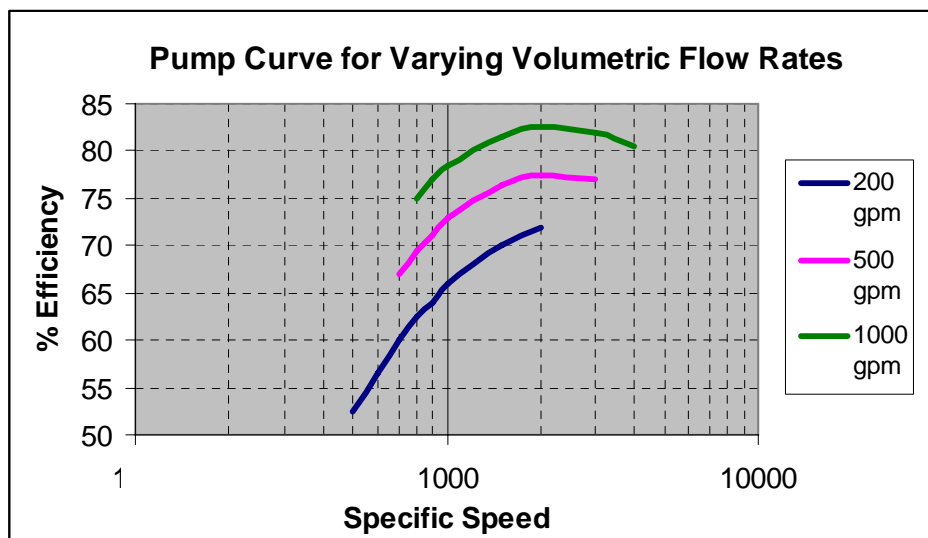
Figure 3: Pump Curve

As shown on the pump curve, the pump efficiency of liquid compression changed slightly with changes in flow rate for different applied stresses. An equation for the efficiency of liquid compression as a function of volumetric flow rate (assuming constant specific speed) was obtained by plotting points read from the pump curve and then fitting a curve in Excel. The curve is shown below in Figure 4 with the equation shown on the graph.
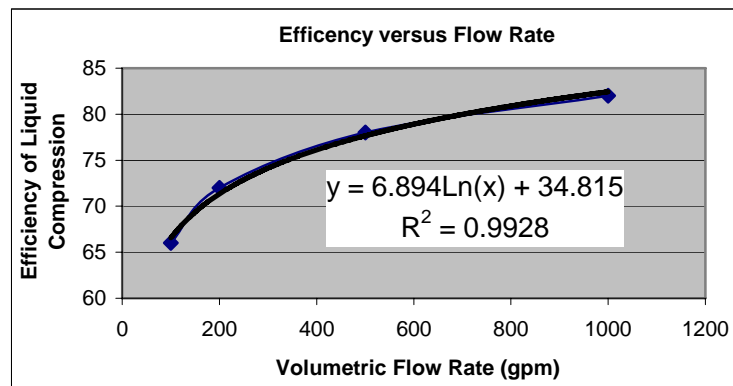
Figure 4: Efficiency of Liquid Compression as a Function of Flow Rate

As also seen on the pump curve, there was a trade-off between pump head and flow rate. The pump was assumed to have a maximum head of 152.135 meters and a maximum flow rate of 1500 gallons per minute (gpm) with a parabolic relationship between these two variables assumed. The following equation shows that relationship.

$$H_p = 152.135\left[1 - (\frac{v_m}{1500})^2\right] \tag{4.1}$$

Where:

H_p = pump head in meters

v_m = volumetric flow rate in gpm

Pump properties are listed in Table 4. The initial water temperature is listed, however this value changed for different stresses applied to the system. Head and flow rate also changed as stresses varied.

Table 4: Pump Test System Properties

System Property	Value	Units
Inlet pipe diameter, D =	5	inches
Initial inlet temperature, T_{in} =	90	^oF
Initial flow rate, v_m =	500	gpm
Inlet pressure, P_{in} =	300	psia
Initial pump head, H_p =	200	psia
Mechanical efficiency, η_m =	0.65	

Heat Exchanger

Phase change behavior was explored using a counter-current steam condenser. Saturated steam entered through the shell side where it condensed before exiting as saturated water. Cooling water entered through the tube side and was heated as the water flowed horizontally through the tubes before exiting. The inlet temperatures and flow rates of the steam and cooling water were specified while calculations determined the outlet temperatures and tube length. While length is an unusual choice, it allowed calculations to be performed without extensive iterations. Thermal expansion between shell and tubes were also neglected.

The condenser was chosen to have no baffles and only one tube pass with tubes positioned at a triangular pitch. The shell diameter, tube pitch/clearance, number of tubes, tube diameter, and tube thickness were determined by choosing a standard combination of those parameters.[46] The condenser materials were chosen to be carbon steel (1% carbon). Some characteristics of the system are summarized in Table 5.

Table 5: Heat Exchanger Test System Properties

System Property	Value	Units
Shell Diameter, D_s =	37	inches
Tube Outside Diameter, $D_{t\,out}$ =	1	inches
Tube Thickness, t =	0.065	inches
Number of tubes	674	
Tube Pitch, P_t =	1.25	inches
Tube Thermal Conductivity,[47] k =	43	W/m/K
Inlet Water temperature, $T_{t\,in}$ =	80	^oF
Inlet Water Pressure, $P_{t\,in}$ =	10	bar
Water Flow Rate (Per Tube), $m_{f\,w}$ =	1	kg/s
Tube Side Fouling Factor, $R_{f,i}$	0.0002	m^2K/W
Inlet Steam Pressure, $P_{st\,in}$ =	50	psia
Initial Inlet Steam Flow Rate, $m_{f\,st}$ =	48	kg/s
Shell Side Fouling Factor, $R_{f,o}$	0.0001	m^2K/W

CALCULATIONS

Calculations were performed for each system in order to determine the system stress and strain variables. Energy balances were performed on each system to allow determination of the inlet and outlet variables for each stream crossing system boundaries. Those variables were then used to calculate the energy and exergy of each stream. The energy and exergy values were then used to determine inlet and outlet energy and exergy as well as the change in exergy for each system.

Steam

All physical properties for the water and steam flow streams were determined using the Excel add-in Water97_v13, version 1.3.[48] This plug-in, authored by Bernhard Spang, calculates transport and thermodynamic properties for both steam and water using IAPWS-IF97, the 1997 standard of the International Association for the Properties of Water and Steam.

The plug-in allowed for the calculation of single-phase properties for density, specific internal energy, specific entropy, specific enthalpy, specific isobaric and isochoric heat capacity, thermal conductivity, and dynamic viscosity.[48] The plug-in was

able to compute properties for states with temperatures between 273.15 and 1073.15 degrees Kelvin and pressures between zero and one thousand bar.

Exergy Calculations

All test systems were statically flowing, steady state systems. There was no chemical reaction or accumulation present. Thus, the exergy of input material streams was calculated using the physical exergy equation stated earlier on a per mass basis as Equation 3.4 and given below as

$$Ex_{in}^{mat} = m_f[H - H_0 - T_0(S - S_0)] \tag{4.2}$$

Where:

Ex_{in}^{mat} = exergy of the input material stream

The only sources of energy into the pipe and heat exchanger systems were the input material streams, so the total exergy into the system equaled the exergy of the input material streams.

The pump had an additional input energy stream, the total electrical energy into the pump. The exergy of electrical energy stream equaled the energy of that stream, since the entire stream had the potential to do work. Thus, the total input exergy to the pump equaled

$$Ex_{in}^{pmp} = W_{in}^{pmp} + Ex_{in}^{mat} \tag{4.3}$$

Where:

Ex_{in}^{pmp} = input exergy into pump

W_{in}^{pmp} = total electrical energy into pump

The exergy out of each system simply equaled the exergy of the output material stream:

$$Ex_{out}^{mat} = m_f[H - H_0 - T_0(S - S_0)] \tag{4.4}$$

Where:

Ex_{out}^{mat} = exergy of the input material stream

Energy Balances

Steam and Water Pipe

The water and steam pipe systems consisted of a pipe and its associated material flows, an inlet and outlet steam stream or an inlet and outlet water stream. Each system operated at steady state and thus the energy balance can be written as:[44]

$$\Delta(H + \frac{1}{2}u^2 + zg) \cdot m_f = Q + W \tag{4.5}$$

Where:

H = stream enthalpy

u = stream velocity

z = elevation

g = gravitational acceleration

m_f = stream mass flow rate

Q = rate of heat addition or removal

W = rate of work addition or removal

Each pipe was assumed to be horizontal with no elevation changes. Kinetic energy effects were neglected since velocity changes were assumed to be minimal. The only work present was work lost overcoming friction effects and the heat rate associated with the system was any heat lost due to transfer to the environment. The energy balance thus reduced to:

$$\Delta(H) \cdot m_f = Q + W \tag{4.6}$$

The preceding equation was used to determine the outlet conditions (outlet enthalpy) of the fluid after pressure drop along the pipe length, heat transfer to the surroundings, and losses associated with friction were determined.

The pressure drop along the pipe length due to friction between the process steam and the pipe wall were calculated using the Darcy-Weisbach equation given below:[49]

$$\Delta P_f = \frac{f v_{in}^2 L \rho_{in}}{2D_{in}} \tag{4.7}$$

Where:

ΔP_f = pressure drop due to friction

f = friction factor from the Churchhill equation

L = pipe length

v_{in} = inlet fluid velocity

ρ_{in} = inlet fluid density

D_{in} = inside pipe diameter

The velocity in the pipe was determined from:

$$v_{in} = \frac{4m_f}{\pi D_{in}^2 \rho_{in}}$$ (4.8)

To simplify calculations, it was ensured that the flow in each pipe was in the fully developed turbulent range, i.e. the Reynolds number, Re, was higher than 4000.[49] The Reynolds number was calculated from the following relation.

$$Re_{in} = \frac{D_{in} v_{in} \rho_{in}}{\mu_{in}}$$ (4.9)

Where:

Re_{in} = inlet Reynolds Number

μ_{in} = inlet fluid viscosity

The pipe friction factor was calculated using the Churchhill equation. The Churchhill equation was chosen because it allowed calculation over a wide range of Reynolds numbers within requiring iteration. The Churchhill equation is shown below.[50]

$$f = 2\left[\left(\frac{8}{Re_{in}}\right)^{12} + \frac{1}{(A+B)^{\frac{3}{2}}}\right]^{\frac{1}{12}}$$ (4.10)

With:

$$A = 2.457 \ln\left[\frac{1}{\left[(\frac{7}{Re_{in}})^{0.9} + \frac{0.27\varepsilon}{D_{in}}\right]}\right]$$ (4.11)

$$B = \left(\frac{37530}{\text{Re}_{in}}\right)^{16} \tag{4.12}$$

Where:

f = Fanning friction factor

ε = pipe roughness

The heat loss due to heat transfer through the pipe wall to the atmosphere was determined by treating the pipe as a composite plane wall. Interfacial contact resistance was neglected, however the temperature profile of the fluid within the pipe was not considered uniform. The inlet temperature of the fluid was assumed to be the temperature at the center of the pipe and the inlet heat transfer coefficient, h_i, was used to determine the fluid temperature at the inside pipe wall. The heat transfer rate due to heat transfer from the pipe center to the wall, through the wall, and from the outside wall to the atmosphere was determined using the following equation:[51]

$$Q_h = \frac{(T_{in} - T_0)}{\left[\dfrac{1}{4\pi D_{in} L h_i} + \dfrac{\ln\left(\dfrac{D_{in} + 2t}{D_{in}}\right)}{2\pi k_w L} + \dfrac{1}{2\pi(D_{in} + 2t)L h_{\text{inf}}}\right]} \tag{4.13}$$

Where:

Q_h = heat transfer rate from pipe to atmosphere

T_{in} = inlet fluid temperature

L = pipe length

h_i = fluid heat transfer coefficient

t = pipe wall thickness

k_w = thermal conductivity of pipe

The fluid heat transfer coefficient was calculated using various heat transfer and transport properties of fluid stream including the Reynolds' number, Prandtl number (Pr), and the Nusselt number (Nu). The Prandlt number was calculated from the following correlation:[46]

$$Pr = \frac{C_p \mu_{in}}{k_{in}} \tag{4.14}$$

Where:

C_p = heat capacity of fluid

Valid for Prandlt numbers between 0.7 and 100, the Dittus-Boelter equation given below[46] was used to calculate the Nusselt number.

$$Nu = 0.023(Re)^{0.8}(Pr)^n \tag{4.15}$$

Where:

n = exponent which equals 0.3 for cooling the fluid, 0.4 for heating

Once the Nusselt number was calculated, the fluid heat transfer coefficient, h_i, was determined from the following correlation:[46]

$$h_i = \frac{k_{in} Nu}{D_{in}} \tag{4.16}$$

Water Pump

The water pump system consisted of the water pump, pump motor, and associated fluid streams. Energy was input into the water pump system via electricity to the pump and energy associated with the flow of water into the pump. Energy was removed from the system via the exiting water stream. Since the system operated at steady state with one material entrance and one exit, the energy balance was the same as for the pipe test system, as shown in Equation 4.5.

Negligible elevation change occurred within the system, thus potential energy terms were eliminated. The pump was assumed to be adiabatic, so heat transfer to the surroundings was neglected. It was assumed that the inlet and exit pipes were sized to prevent large changes in velocity, so kinetic energy terms were neglected as well. The rate of work term was due to the addition of shaft work into the system, W_s, thus, the preceding equation simplified to:

$$W_s = m_f \Delta H \tag{4.17}$$

Inlet conditions (temperature and pressure) as well as the outlet pressure were known. However, the outlet temperature and shaft work rate were not known so the energy balance could not be used to determine the stream outlet enthalpy. However, if the pumping process was reversible as well as adiabatic, the process would be isentropic and thus the outlet entropy of the water stream would equal the inlet entropy of the water stream.[44] Fixing the outlet entropy would allow the determination of the isentropic outlet enthalpy and the isentropic shaft work, W_s*(isentropic),* from the energy balance. However, the actual pumping process was not completely reversible or isentropic, so the calculated shaft work would be the minimum work required to produce the desired increase in pressure. Since pumps cannot compress with 100% efficiency, the actual shaft work required was calculated with knowledge of the pump's efficiency as stated in the following equation.

$$\eta_i = \frac{W_s(isentropic)}{W_s} \tag{4.18}$$

Where:

η_i = pump efficiency of liquid compression

However, the preceding method outlined required the knowledge of subcooled liquid properties that are not always available. While these properties were available from steam tables, the Excel plug-in used for these calculations only allowed the determination of enthalpy and entropy if given the temperature and pressure. It would not allow the user to determine the pressure or temperature if given one property and the enthalpy or entropy. Thus, the use of the preceding method would require an extensive iterative process. Since each new stress applied (variable change) would require new iterations, this would quickly become time-prohibitive. Thus, the following property relation for isentropic processes was used as an alternative:[44]

$$dH = VdP \tag{4.19}$$

Thus, the pump energy balance was written as:

$$W_s(isentropic) = (\Delta H)_s = \int_{P_1}^{P_2} VdP \tag{4.20}$$

Where:[44]

$(\Delta H)_s$ = isentropic change in enthalpy of water stream

P_1 = inlet water pressure

P_2 = outlet water pressure

V = volume

For liquids that are not close to their critical point, it can be assumed that volume is independent of pressure and thus integration yields:[44]

$$W_s(isentropic) = (\Delta H_s) = V(P_2 - P_1) \tag{4.21}$$

The actual shaft work was again calculated using the pump efficiency of liquid compression. The volume independent of pressure assumption also allowed the increase in temperature within the pump to be determined from the following equation:[44]

$$dH = C_p dT + v_m(1 - \beta T)dP \tag{4.22}$$

Where:

C_p = specific heat

v_m = volumetric flow rate

β = volume expansivity coefficient

Since liquid properties change little with pressure and the temperature change will be small, this equation was integrated using the assumption that v_m, C_p, and β were constant over the pressure and temperature ranges. This gave[44]

$$\Delta H = C_p(T_2 - T_1) + V(1 - \beta T)(P_2 - P_1) \tag{4.23}$$

Where:

T_1 = inlet water temperature

T_2 = outlet water temperature

The volume expansivity coefficient (with units of inverse Kelvin) was determined using the following correlation, which is valid from –40 to 120°C and for pressures between 0 and 500 MPa:[52]

$$\beta = [A + \frac{B}{C + \Pi}] \cdot 10^{-4} \tag{4.24}$$

With:

$$A = 47.8506 + -0.0812847T + 8.49849 \cdot 10^{-5}T^2 \tag{4.25}$$

$$B = 5.56047 \cdot 10^5 - 0.00376355T + 5.56395T^2 + 0.00559682\Pi T - 27.6522\Pi \quad (4.26)$$

$$C = -4280.67 - 33.915T + 0.365873T^2 - 5.589617 \cdot 10^{-4} T^3 \qquad (4.27)$$

$$\Pi = P + 3.28892 \cdot 10^{-4} P^2 - 2.65933 \cdot 10^{-8} P^3 \qquad (4.28)$$

Where:

P = pressure in bars

T = temperature in Kelvin

The total work into the pump system required the inclusion of another efficiency – the efficiency of the pump motor. To determine the total work into the system, the actual shaft work was divided by the motor efficiency. The energy lost due to motor inefficiencies went into overcoming friction effects within the motor, heat lost to the motor bearings, noise, vibrations, and other sources. Since the pump was adiabatic, it will be assumed that this lost work in the motor did not affect the fluid within the pump.

Heat Exchanger

The heat exchanger system consisted of a counter flowing steam condenser and the associated water and steam inlet and outlet material streams. The hot fluid was steam while the cold fluid was cooling water. Since both outlet temperatures as well as the tube length were not known, the energy balance required at least one iteration. However, iterations were limited to one by using average thermodynamic values and fixing the initial guess for the overall heat coefficient within the typical range. The recommended range is between approximately 700 and 1700 W/m^2/K,[46] thus the initial guess was 1600 W/m^2/K. To calculate the overall heat transfer coefficient, the outside pipe surface was used as a basis, however this choice was arbitrary since the product of heat transfer coefficient times its associated area is equal as shown.

$$\frac{1}{UA} = \frac{1}{U_o A_o} = \frac{1}{U_i A_i} \qquad (4.29)$$

Where:

U = overall heat transfer coefficient

A = heat transfer area

U_o = overall heat transfer coefficient based on outer tube surface

A_o = outer tube surface area

U_i = overall heat transfer coefficient based on inner tube surface

A_i = inner tube surface area

The areas were calculated as follows:

$$A_o = \pi D_o L \tag{4.30}$$

$$A_i = \pi D_i L \tag{4.31}$$

Where:

D_o = tube outside diameter

D_i = tube inner diameter

Since the condenser was a tubular exchanger with no fins or other enhancements, the outside overall heat transfer coefficient was calculated from the following equation. The product of overall heat transfer coefficent and area were later used, but the coefficient itself was not used alone, so it did not matter which of the heat transfer coefficients was calculated.[46]

$$U_o = \cfrac{1}{R_{f,o} + \cfrac{1}{h_o} + \cfrac{t D_i \ln(D_o - D_i)}{k(D_o - D_i)} + \cfrac{D_o}{h_i D_i} + R_{f,i}\left(\cfrac{D_o}{D_i}\right)} \tag{4.32}$$

Where:

$R_{f,o}$ = shell side fouling factor

h_o = outside surface heat transfer coefficient

t = tube thickness

k = tube heat conductivity coefficient

L = tube length

h_i = inner surface heat transfer coefficient

$R_{f,i}$ = tube side fouling factor

The rate of heat transfer between the shell and tube-side process fluids was determined using an energy balance. The heat exchanger was assumed to operate at

steady state. There were two inlet and exit material streams, thus the energy balance became:

$$\sum \left[(\Delta H + \frac{1}{2}u^2 + zg) \cdot m_f \right] = Q + W \tag{4.33}$$

Each process fluid (water and steam) contributed a term to the left side. The condenser was assumed to be horizontal, so there was no elevation change on the tube side. The steam side elevation change as also assumed to be negligible. Kinetic energy effects were neglected for the tube side and for the shell side, since the inlet and outlet pipes were assumed to be sized to prevent large velocity changes. The condenser was assumed to be well insulated from its surroundings, thus heat transfer to the surroundings was neglected and there was no work input into the system. Therefore, the energy balance reduced to the following equations for the tube and shell side.

$$Q = (m_f \Delta H)_{steam} = (m_f \Delta H)_{water} \tag{4.34}$$

Where;

Q = heat transferred between the hot and cold streams

This rate of heat transfer was also expressed using the following equation:[51]

$$Q = UA\Delta T_{LM} \tag{4.35}$$

Where:

ΔT_{LM} = log mean temperature difference

The log mean temperature difference was used in place of the temperature difference between the hot and cold streams because the temperature difference between the streams varied with position within the exchanger while the log mean temperature difference provided an appropriate mean value. It was calculated for counter-flow exchanger using the following equation:[51]

$$\Delta T_{LM} = \frac{(T_{h,o} - T_{c,i}) - (T_{h,i} - T_{c,o})}{\ln\left(\dfrac{T_{h,o} - T_{c,i}}{T_{h,i} - T_{c,o}}\right)} \tag{4.36}$$

Where:

$T_{h,o}$ = outlet hot fluid (shell side) temperature

$T_{c,i}$ = inlet cold fluid (tube side) temperature

$T_{h,i}$ = inlet hot fluid (shell side) temperature

$T_{c,o}$ = outlet cold fluid (tube side) temperature

In order to calculate the flow and heat transfer properties of the tube side, average thermodynamic properties were used. Since properties such as density, viscosity, and thermal conductivity differed along the length of the tube, as the water temperature increased, these properties changed. The tube side flow and heat transfer properties were characterized using dimensionless numbers. The Reynolds number was calculated as follows, where the mass flow rate represented the flow through one tube:

$$\mathrm{Re}_t = \frac{4 m_f}{\pi D_{in} \mu_{avg}}$$
(4.37)

Where:

Re_t = Tube side Reynolds number

μ_{avg} = average viscosity of tube fluid

The Prandtl number was calculated using the following relation based on average fluid properties.[51]

$$\mathrm{Pr}_t = \frac{Cp_{avg} \mu_{avg}}{k_{avg}}$$
(4.38)

Where:

Pr_t = tube side Prandtl number

Cp_{avg} = average heat capacity of tube side fluid

k_{avg} = average thermal conductivity of tube side fluid

Once the Prandtl and Reynolds numbers were known, the Nusselt number was calculated using the following equation. The 0.4 power for the Prandtl number was due to the fact that the tube side fluid was being heated.[51]

$$Nu_t = 0.023\, \mathrm{Re}_t^{4/5}\, \mathrm{Pr}_t^{0.4}$$
(4.39)

Where:

Nu_t = tube side Nusselt number

Once the Nusselt number was calculated, the tube side heat transfer coefficient was determined using:

$$h_i = \frac{Nu_t k_{avg}}{D_{in}} \tag{4.40}$$

While the temperature at the tube outlet was not known, the outlet pressure was calculated by determining the pressure drop through each tube. The pressure drop was calculated using:[51]

$$\Delta P_t = \frac{1.2 f_t G^2 L}{2 g_c \rho_{avg} D_i \phi} \tag{4.41}$$

Where:

f_t = tube side friction factor

G = mass flow rate per unit area

g_c = gravitational constant

ϕ = viscosity correction factor

The friction factor and mass flow rate per unit area were calculated as follows, where the mass flow rate is on a per tube basis:[51]

$$f_t = [1.82 \log(Re_t) - 1.64]^{-2} \tag{4.42}$$

$$G = \frac{4 m_f}{\pi D_{in}^2} \tag{4.43}$$

The viscosity correction factor adjusted for the fact that the viscosity within the tube differed from the viscosity on the wall of the tube. It was calculated as follows:[51]

$$\phi = 1.02 \left(\frac{\mu_{avg}}{\mu_{w,t}} \right)^{0.14} \tag{4.44}$$

Where:

$\mu_{w,t}$ = viscosity of tube-side fluid at wall

The wall viscosity was based on the pressure and substance of the tube-side fluid however the temperature was higher due to the presence of the hot fluid on the shell side.

Since the shell-side fluid was condensing, the shell-side temperature remained close to constant, thus the wall temperature was calculated as

$$T_{w,t} = \frac{(T_{t,avg} + T_s)}{2}$$ (4.45)

Where:

$T_{w,t}$ = tube side wall temperature

$T_{t,avg}$ = average temperature within tube

T_s = shell side steam temperature

Shell-side calculations begin with determining an effective diameter for the shell. Not all the volume within the shell was available for flow since some was taken up by the presence of tubes. The effective diameter was[46]

$$D_e = \frac{4(P_T^2 \sqrt{3} - \pi D_o^2 / 8)}{\pi D_0 / 2}$$ (4.46)

Where:

D_e = effective shell diameter

P_T = tube pitch

The area of the shell was calculated as:

$$A_s = \frac{D_s CL}{P_T}$$ (4.47)

Where:

C = tube clearance (pitch minus tube outer diameter)

D_s = shell diameter

Once the area was calculated, the steam mass flow rate per area was calculated as:

$$G_s = m_f / A_s$$ (4.48)

Where:

G_s = shell mass flow per unit area

The Reynolds number for the condensing steam was calculated using the following equation:[53]

$$\text{Re}_s = \frac{D_o G_s \rho_l}{\mu_l \rho_g} \qquad (4.49)$$

Where:

Re_s = shell side Reynolds number

ρ_l = condensed density

μ_l = condensed viscosity

ρ_g = shell side vapor phase density

The Prandtl number for condensing water was calculated using a correlation reported by Gambill:[53]

$$\text{Pr}_s = 10^{\wedge}[\frac{0.0244(H_g - H_l)MW}{T_s} - 2.2] \qquad (4.50)$$

Where:

Pr_s = shell side Prandtl number

H_g = shell side enthalpy of vapor state

H_l = shell side enthalpy of condensed state

MW = molecular weight of shell side fluid

The Nusselt number for a condensing stream was calculated using an equation proposed by Taborek[53]

$$Nu_s = 0.3\,\text{Re}_s^{0.6}\,\text{Pr}_s^{0.4}\sqrt{\left(\frac{\rho_l}{\rho_g + 1}\right)} \qquad (4.51)$$

The shell side heat transfer coefficient was then calculated as:[53]

$$h_o = \frac{Nu_s k_g}{D_e} \qquad (4.52)$$

Where:

k_g = shell side vapor phase heat conductivity

The outlet pressure of the condensing steam was calculated by determining the liquid phase and vapor phase pressure drops and then combining them using the Chisholm correlation:[53]

$$\frac{\Delta P_s}{\Delta P_l} = 1 + (Y^2 - 1)\left[Bx_g^{(2-n)/2}(1 - x_g)^{(2-n)/2} + x_g^{2-n}\right] \tag{4.53}$$

Where:

ΔP_s = shell side pressure drop

ΔP_l = shell side liquid pressure drop

Y = Chisholm parameter

B = Blasius parameter

x_g = gas phase mass flow fraction

n = power of the friction factor/Reynolds number relationship

Since the fluid was transitioning from all vapor to all liquid, x_g was assumed to be 0.5 to obtain an average pressure drop for the entire shell side. For two-phase cross-flow horizontal flow, B equals 0.75 while n equals 0.46. The Chisholm parameter could thus be stated as:[46]

$$Y^2 = \frac{\Delta P_g}{\Delta P_l} \tag{4.54}$$

Where:

ΔP_g = shell side vapor pressure drop

Substituting those values, the Chisholm correlation simplified to:

$$\Delta P_s = 0.398\Delta P_l + 0.602\Delta P_g \tag{4.55}$$

The vapor pressure drop was calculated from a modified Fanning equation proposed by Grimison for fluid flow across the shell side of a shell and tube exchanger. The correlation includes the number of rows within the exchanger. For this exchanger, there were 29 rows of tubes.[51]

$$\Delta P_g = \frac{2.2 f_g' N_R G_s^2}{\rho_g \phi_g} \tag{4.56}$$

Where:

f_g' = shell side vapor phase friction factor

N_R = number of tube rows within exchanger

ϕ_g = shell side vapor phase viscosity correction factor

Similarly, the liquid pressure drop was calculated using

$$\Delta P_l = \frac{2.2 f_l' N_R G_s^2}{\rho_l \phi_l} \quad (4.57)$$

Where:

f_l' = shell side liquid phase friction factor

ϕ_l = shell side liquid phase viscosity correction factor

The shell side vapor phase friction factor was calculated from:[51]

$$f_g' = b\left(\frac{D_o G_s}{\mu_g}\right)^{-0.15} \quad (4.58)$$

Where:

μ_g = shell side vapor phase viscosity

b = pitch coefficient

The shell side liquid phase friction factor was

$$f_l' = b\left(\frac{D_o G_s}{\mu_l}\right)^{-0.15} \quad (4.59)$$

Since this exchanger had staggered tubes at a triangular pitch, the b factor was calculated as[51]

$$b = 0.23 + \frac{0.11}{(P_T / D_o - 1)^{1.08}} \quad (4.60)$$

The shell side vapor phase viscosity correction factor was calculated similar to the tube side viscosity correction factor.

$$\phi_g = 1.02\left(\frac{\mu_g}{\mu_{w,g}}\right)^{0.14} \quad (4.61)$$

Where:

$\mu_{w,g}$ = viscosity of shell side vapor phase at wall

The wall viscosity was based on the pressure of the shell-side fluid with an average temperature based on the tube side and shell-side temperatures. The liquid phase viscosity correction factor was:

$$\phi_l = 1.02 \left(\frac{\mu_l}{\mu_{w,l}} \right)^{0.14} \tag{4.62}$$

Where:

$\mu_{w,l}$ = viscosity of shell side liquid phase at wall

Once the outlet steam pressure was calculated, the outlet steam temperature could be determined since the outlet condensate was saturated water. Knowing the outlet temperature and pressure, the outlet shell side enthalpy could be determined. This enthalpy was used in association with the inlet steam enthalpy and the steam flow rate to determine the heat rate necessary to condense the steam. From this heat rate, the outlet enthalpy of the cooling water stream could be determined (again using the inlet cooling water enthalpy and mass flow rate). The outlet cooling water temperature was then determined from the outlet enthalpy, allowing the calculation of a ΔT_{LM} for the exchanger. This log mean temperature difference and the heat rate were used to determine a $U_o A_o$ value using equation 4.35. Since U_o could be determined from equation 4.32, the length of the exchanger tubes could now be calculated.

However, this calculation procedure assumed an average temperature for the tube-side fluid. Since the inlet and outlet temperatures of the cooling water were now known, a second iteration was made using this more accurate average temperature (the outlet temperature changed slightly during the second iteration).

STRESSES APPLIED

"Stresses" were applied to systems by changing the inlet temperature, pressure, and mass flow rates for different system streams. Since variable changes resulted in different energy loads being input or applied to each system, these changes allowed the behavior of each system to be analyzed for a range of energy loads. The systems were allowed to undergo incremental increases in each of the variables and the stress and strain variables were recalculated for every new system condition. Table 6 shows the initial value and variable range for each of the test systems.

Table 6: Ranges of Applied Stresses for Test Systems

System	Inlet Variable	Initial Value	Maximum Value
Steam Pipe	Steam Mass Flow Rate	8 kg/s	28 kg/s
	Steam Temperature	500°F	1000°F
	Steam Pressure	100 psia	300 psia
Water Pipe	Water Mass Flow Rate	15 kg/s	60 kg/s
	Water Temperature	100°F	280°F
	Water Pressure	50 psia	600 psia
Water Pump	Volumetric Flow Rate	250 gpm	750 gpm
	Water Temperature	90°F	390°F
Heat Exchanger	Steam Mass Flow Rate	50 kg/s	75 kg/s
	Cooling Water Temperature	80°F	130°F

SUMMARY

Test systems were chosen to allow the resilience concept to be developed and demonstrated on specific process systems. The properties and parameters for each of the test cases – a steam pipe, a water pipe, a water pump, and a heat exchanger – were outlined. Calculations were outlined for each system that will allow the determination of system strain and stress variables from system energy and exergy balances. Finally, stresses applied to each system in the form of incremental variable increases were presented.

CHAPTER V
RESULTS AND ANALYSIS

Using the calculations and stress variations presented in the last chapter, a series of stress and strain variables were obtained for each of the four test systems. This chapter will present these data in graphical form for each system and variable change as well as combined graphs showing all stresses applied to each system. Graphs were created in Excel to show the behavior of system stress versus system strain for each example over a range of parameters.

CHARACTERISTIC SYSTEM CURVES
Steam Pipe

The different steam pipe stresses were obtained by changing the mass flow rate, temperature, and pressure independently. The base case for the steam pipe was a pipe at 500^oF and 100 psia containing 8 kg/s steam. The first graph in Figure 5 shows the mass flow rate changed from 6 kg/s to 28 kg/s in 2 kg/s increments while the temperature and pressure were held constant at 500^oF and 100 psia. The second graph (Figure 6) shows the steam temperature changing from 500^oF to 1000^oF in 25^oF increments while the mass flow rate was held constant at 8 kg/s and the pressure was held at 100 psia. The third graph (Figure 7) shows the steam pressure changing from 100 psia to 300 psia in 20 psia increments while the temperature and mass flow rate are held constant at 500^oF and 8 kg/s respectively.
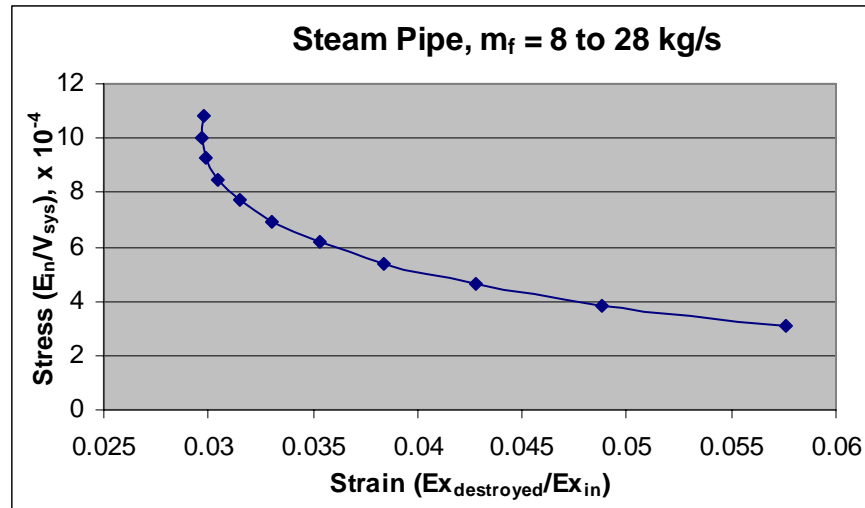
Figure 5: Characteristic System Curve for Steam Pipe, Changing Mass Flow Rate
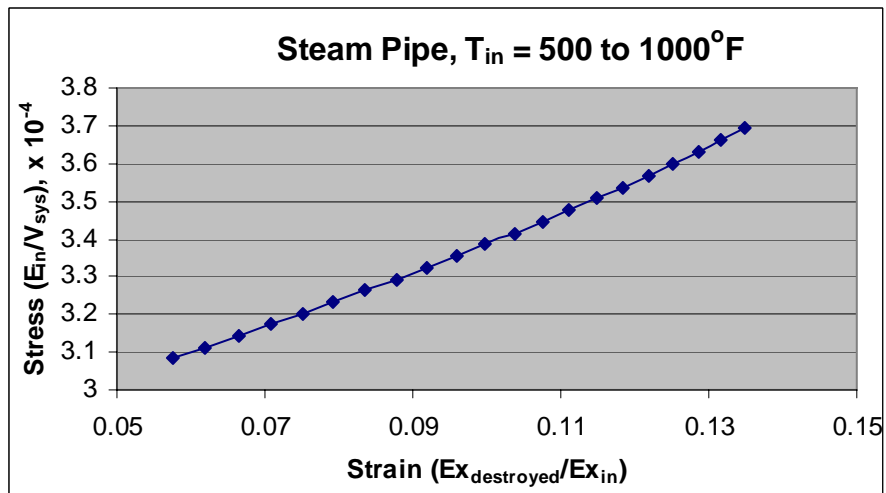
Figure 6: Characteristic System Curve for Steam Pipe, Changing Temperature
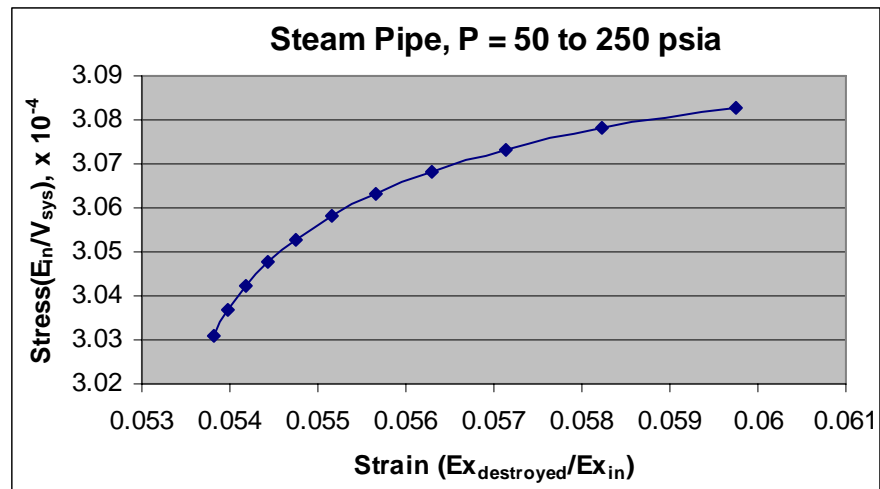
Figure 7: Characteristic System Curve for Steam Pipe, Changing Pressure

The graphs show different shapes – the relationship between stress and strain is different for the three cases. It can be seen that all stress scales begin at approximately 30,000 kJ/m^3-s, however the maximum stress is different for all three cases and the strain ranges differ. The mass flow graph shows an inverse relationship between stress and strain with the initial stress increasing as mass flow increases while the strain decreases with the increasing stress. The slope of the curve also increases as the strain increases – while the slope starts gradually increasing, the slope increases until the curve slope appears close to vertical. The physical explanation for these effects is that as the mass flow rate increases, the friction factor (*f*) increases: however, this increase levels off at the end of the mass flow rate range. So while each higher flow rate point destroys more exergy by transforming mechanical flow energy into thermal energy, the system destroys proportionally less exergy as the flow rate is increased due to the smaller percentage increase in the friction factor. Therefore, the system operates at higher efficiency levels as the mass flow rate increases, but if the system has been designed to operate at lower efficiencies, a higher efficiency may result in more exergy than the system has been designed to withstand. At higher flow rates, the system has (percentage-wise) more potential to do work on its surroundings than originally anticipated.

The temperature and pressure curves show a direct relationship between stress and strain, however there are some other significant differences. The temperature curve shows a somewhat linear trend with the slope appearing to increase very gradually, while the pressure curve shows closer to a polynomial or power relationship between stress and strain with the slope decreasing as the stress increases.

For the temperature curve, as the stress increases, so does the strain value. While this trend remains remarkably consistent throughout the investigated temperature range, toward the high end of the range the strain values begin to increase at a slightly slower rate resulting in an increase in the curve slope. The decline in the rate of increase for the strain values can be explained by observing that while the pipe does dissipate a higher amount of energy due to heat loss to the atmosphere, the amount of energy added to the system by the higher inlet temperature is increasing at a faster rate. Thus, while the percentage of exergy lost still increases for higher temperatures, it grows at an increasingly lower rate. Thus, the amount of exergy contained within the system is less than what would be predicted by the initial displayed trend.

For the changing pressure curve, the stress and strain both decrease as higher pressures are applied. The stress decreases due to the decreasing inlet steam enthalpy while the strain decreases in part due to the decreasing pressure drop within the system. However, as the pipe experiences higher pressures, the decreasing strain values begin to level off due to a leveling off of the velocity within the pipe. As the inlet steam density decreases, the velocity decreases, but this effect yields diminishing returns as the density moves to higher values. Thus, while the system efficiency increases as the stress decreases, the decreasing rate results in the system containing more exergy (and hence more potential to do work in the system or its surroundings) at lower stress values than would be predicted by the initial trend.

Water Pipe

Variables changed for the water pipe also included water mass flow rate, inlet water temperature, and inlet water pressure. The water base case consisted of a water

pipe with 15 kg/s water flow held at 50 psia and 100°F. In the first graph (Figure 8), the mass flow rate is changed from 15 kg/s to 60 kg/s in 5 kg/s increments while the temperature and pressure were held constant at 100°F and 50 psia. The water temperature in the second graph (Figure 9) is changing from 100 °F to 280°F in 10°F increments while the mass flow rate remained at 15 kg/s and the pressure was held constant at 50 psia. Figure 10 shows the steam pressure varying from 50 psia to 600 psia in 50 psia increments while the temperature remained a constant 100°F and the mass flow rate remained at 15 kg/s.
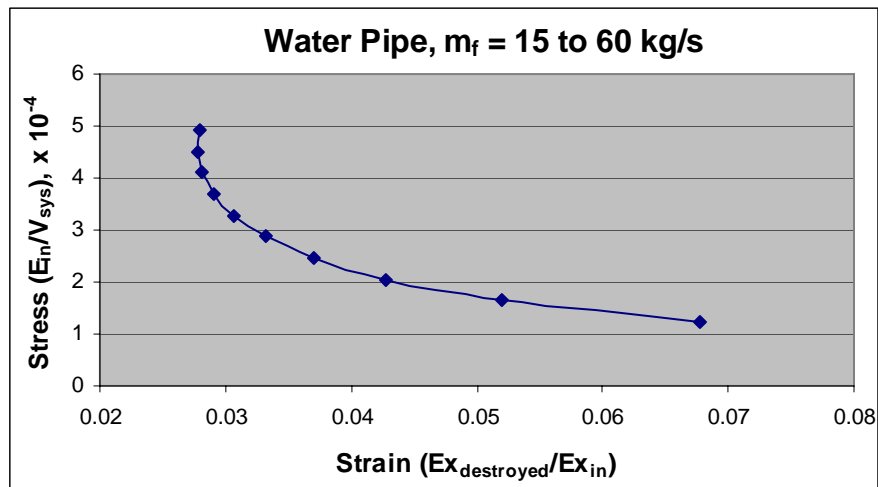
Figure 8: Characteristic System Curve for Water Pipe, Changing Mass Flow Rate
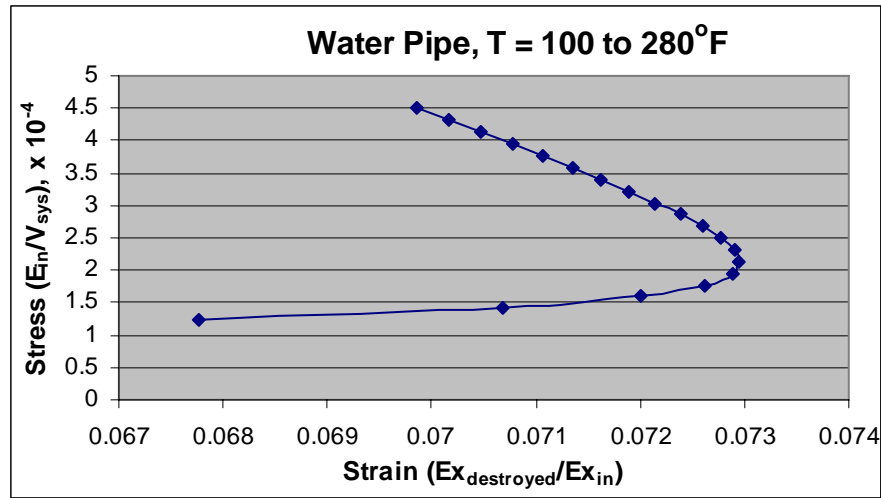
Figure 9: Characteristic System Curve for Water Pipe, Changing Temperature
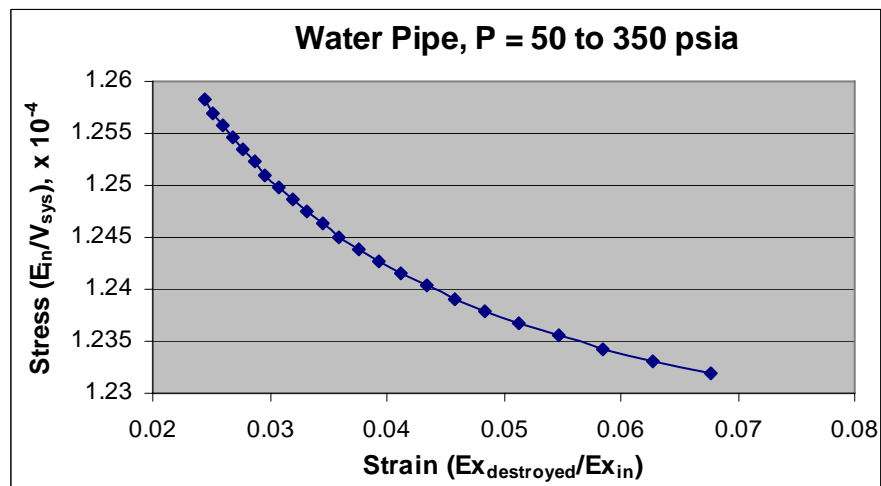
Figure 10: Characteristic System Curve for Water Pipe, Changing Pressure

Again, the curves display similarities and differences. All three curves begin at an initial stress value of approximately 12,000 kJ/m^3-s, however the mass flow and pressure curves display an inverse relationship between stress and strain while the temperature curve shows an initially direct relationship changing to an inverse relationship. The water temperature curve shows a new feature – an inflection point. The

strain first increases as the stress increases – after reaching a maximum strain around 0.073, the strain then decreases as the stress increases. This inflection point shows a clear change in the system's behavior. The reason for the inflection point is the relation of the process conditions to the reference conditions. At the initial lower temperature, the process operates very close to the reference temperature and thus the exergy within the process is minimal. As the process temperature increases, the exergy within the process also increases, but at a higher rate as the temperature moves further from the reference temperature. The exergy destroyed by the process is also increasing due to greater amounts of heat lost to the atmosphere – the rate of exergy lost increases as the temperature is increased. The initial increase in strain occurs because the increase in the amount of exergy lost has more effect on the strain value than the increase in overall exergy into the process. As the exergy into the process further increases, the trend reverses with the added exergy into the process having more of an effect on the strain value than the additional lost exergy.

The mass flow curve shows a gradually increasing slope as the strain decreases with increasing stress. It is worth noting that the water mass flow curve trend closely resembles the steam mass flow curve with curve slope increasing up until the curve appears close to vertical. As the mass flow rate increases, the pipe pressure drop also increases and the friction factor decreases slightly. The heat dissipated to the atmosphere remains approximately constant with the flow increases, however the velocity within the pipe increases. The amount of exergy destroyed by the process increases slightly with flow rate increases due to higher friction losses, but this rate of increase is less than the rate that exergy is added to the system by additional mass flow. Thus, the percentage of exergy lost decreases, resulting in higher mass flow rate systems containing proportionally more exergy than the initial system and thus having more potential to do work in the system.

The water pressure curve shows a gradually increasing slope as the stress increases, however this trend is different than the steam pressure trend. The water pipe stress increases with higher pressures while the strain decreases. The rate of decrease in

the strain value lessens as the pressure increases – a reason for this includes an approximately constant amount of exergy destroyed at each pressure. With the amount of exergy remaining approximately constant, the percentage decreases due to higher initial amounts of exergy within the process at higher pressures. Thus, the system has proportionally more exergy than initially expected at higher pressures.

Water Pump

For the water pump system, the water volumetric flow rate and inlet water temperature were varied. Since the volumetric flow rate and pump head are related, the pump head will also vary with the volumetric flow rate. For the water temperature variation in Figure 11, the mass flow rate will vary slightly due to changes in water density with temperature changes. The base case for the pump was an inlet water temperature of $90^{o}F$ and volumetric flow rate of 250 gpm. The temperature change case consisted of the temperature varied from $90^{o}F$ to $390^{o}F$ while the volumetric flow rate was fixed at 250 gpm. For the volumetric flow rate case (Figure 12), the inlet water temperature was fixed at $90^{o}F$ while the flow rate was varied from 250 to 750 gpm.
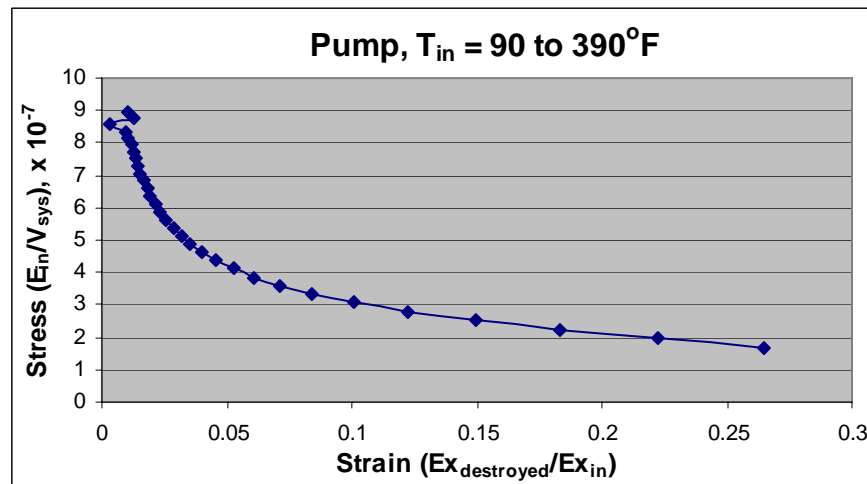
Figure 11: Characteristic System Curve for Water Pump, Changing Temperature
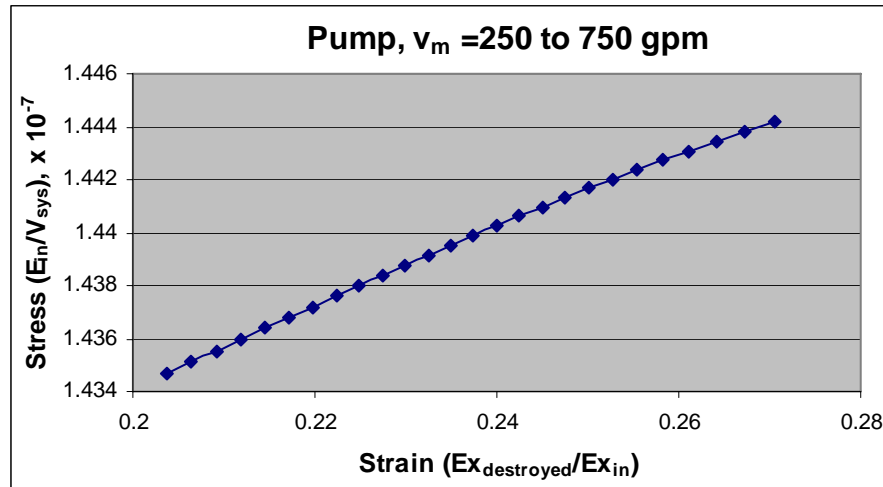
Figure 12: Characteristic System Curve for Water Pump, Changing Volumetric Flow Rate

While the temperature curve shows an inverse relationship between system stress and strain, the volumetric flow curve shows a direct relationship. Both curves begin around a stress value of 15,000,000 kJ/m^3-s; however, the volumetric flow curve shows a direct, close to linear relationship with a very gradually decreasing slope as the mass flow rate decreases (and stress increases). The stress increases with decreasing mass flow rate due to the manner in which pump volume is defined – the volume is defined by the volumetric flow rate divided by the pump's specific speed (constant for this example). Thus, the volume decreases for decreasing mass flow rates resulting in a slight increase in the pump's stress despite the decrease in total energy into the pump. The gradually decreasing slope can be partially attributed to the decrease in pump efficiency with lower mass flow rates – the volumetric flow rate and efficiency are related by a natural log trend. Thus, the pump begins to destroy a higher percentage of the input exergy.

The temperature curve displays an inverse relationship where the strain decreases as the stress increases and the slope increases until the curve deviates from the consistent trend and the data points show significant scatter from the previously-seen power law

relationship. The reason for the scatter is the onset of a phase change and cavitation – the water beginning to change to vapor at higher temperatures. The onset of cavitation represents an unsafe operating point, so it is encouraging that the behavior of the curve indicates significant deviations from the previously displayed trend.

Heat Exchanger

For the heat exchanger system, two variables were chosen for stresses – one involving tube side properties, the inlet water temperature, and one for shell side properties, the steam mass flow rate. The base case for the heat exchanger was steam flowing at 50 kg/s and an inlet water temperature of 80^oF. When the steam rate was varied from 50 kg/s to 75 kg/s in 1 kg/s increments, the water temperature was held constant at 80^oF. The steam mass flow rate was held at 50 kg/s when the steam temperature was varied from 80 to 130^oF in 2^oF increments. Figure 13 shows the mass rate changing, while Figure 14 shows the changing water temperature.
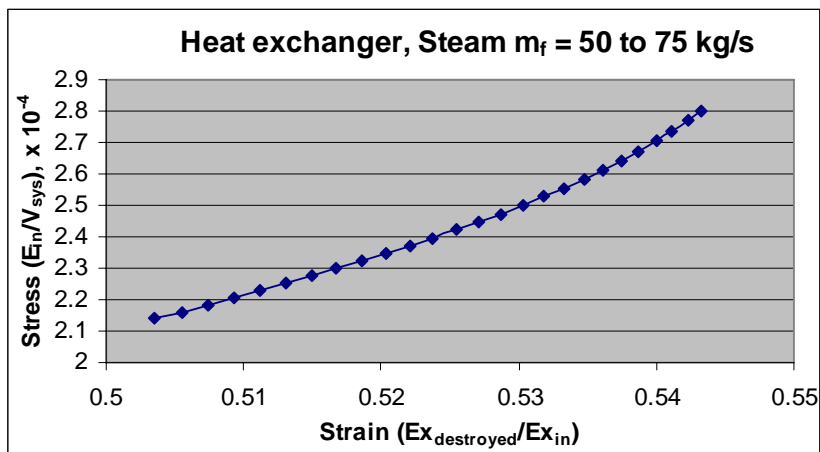
Figure 13: Characteristic System Curve for Heat Exchanger, Changing Steam Mass Flow Rate
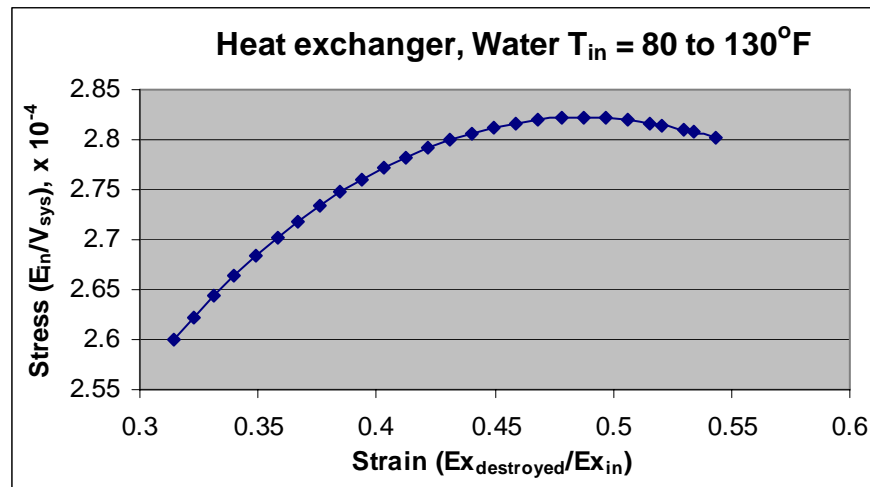
Figure 14: Characteristic System Curve for Heat Exchanger, Changing Inlet Water
Temperature

Again, the curves show different shapes with some similarities. The stress and
strain ranges for the temperature case are wider than those for the mass flow range. One
possible reason for the difference in shape is due to the fact the mass flow stress changes
were applied to the shell side fluid, while the temperature stress changes were applied to
the tube side fluid. The changing inlet water temperature curve shows an increasing
slope that plateaus, and then begins to decrease – the graph features a maximum stress
value midway through the range. One reason for this maximum is that there is a balance
between the energy into the exchanger and the volume of the exchanger – as the inlet
water temperature increases, the volume required (length of tubes) increases as well.
Since these variables do not increase at the same rate, a maximum point can occur since
the variables are divided by each other. For this example, as the cooling water
temperature increases towards the range maximum of $130^{o}F$, the exchanger length has to
increased a great deal due to the loss of temperature driving force between the cold and
hot streams. Thus, towards the end of the range, the volume is increasing faster than
energy into the exchanger. The strain also decreases at an increasing rate as the

temperature increases due to the fact that a lower portion of the outlet exergy has been transferred from the steam stream.

The changing steam mass flow rate curve shows a direct, near linear relationship with a gradually increasing slope. The stress into the system decreases with increasing flow rate: while the energy into the system increases for higher flow rates, the length of the exchanger also increases resulting in a net stress decrease. The strain into the system also decreases with increasing flow rate: the higher flow rate results in higher throughput of exergy (smaller percentage of total exergy in system is destroyed).

TRENDS AND SIGNIFICANCE

The graphs show similar behavior for different systems, with all observations made on a qualitative basis. While some similar behavior has been observed for different stresses to the same system, some of the stresses still show radically different behavior for the same system and the exact system stress and strain ranges differ for different types of system changes.

So what is the significance of these graphs? From the point of view of determining resilience, it would be desirable for these graphs to show where the system transitions from a resilient to a non-resilience behavior region. For linearly elastic material stress-strain curves, the resilient region is characterized by a linear slope (linearly proportional relationship between stress and strain), while the transition to non-linear behavior occurs when the slope deviates from that linear behavior. While some of these graphs do show an initial linear region, it is likely too restrictive to require linearity for resilient behavior. However, all curves show changing trends between stress and strain, so there is likely some predictive ability to determine the expected behavior of the system. The most straightforward predictive method would be some specified relationship between stress and strain in the resilient region (for example, exponential, polynomial, linear, etc). If there was some form of expected behavior, onset of non-resilience would be when the curve deviates from that specified relationship.

Stress and Strain Variable Changes

For the regions within the predicted or specified relationship, the relative storage and dissipation of energy potential or exergy within the system is expected to be proportional to the added or decreased energy "concentration" within the system. However, when the slope increases more than expected, the relative storage and dissipation of exergy is not proportional (as expected) to the stress, or energy "concentration." For directly related stress and strain where the added energy concentration is increasing faster than the expected relative exergy destruction by the system, two possible explanations exist – the first is that the system is simply operating more efficiently. From a sustainability perspective, this would be a desired system state. Exergy destruction is essentially wasted energy potential, so systems that conserve exergy are both more sustainable as well as more cost effective and efficient. However, another possible explanation is that the exergy destruction modes of the system could be overwhelmed. Since exergy destruction is a manner in which the system can shed excess energy load, if the capacity of these modes is reached, the system will have to store the added energy load. However, the system will eventually reach the upper bound of its energy storage capacity and then a failure could occur. For inversely related stress and strain variables with a higher than expected increase in slope, the exergy destruction is not decreasing as much as expected. An explanation for this is that the system may be dissipating the excess energy load by destroying more exergy than normal. Exergy destruction modes are a way in which the system can "rid" itself of its energy load. Thus, the system could be dissipating more exergy in an attempt of stay within its energy capacity range. However, at some point the system will not be able to dissipate or store the addition energy load and then a failure may occur. For directly related regions showing more than expected decreases in the expected slope, the relative storage and dissipation of exergy are again not proportional as expected to the energy "concentration." The added exergy destruction is increasing faster than the relative added energy concentration.

For the graphs showing inflection points or maximum and minimum points, these are clear points where the behavior of the system is changing, as the slope of the curve is changing from increasing to decreasing or vise versa. Since these points indicate the system is moving from dissipating proportionally more exergy to conserving proportionally more exergy (or vise versa), these points will become important as the system's resilient behavior is quantitatively analyzed.

Further Safety Implications

Again, since this concept is being explored with the goal of designing safer systems, the specific safety implications of these results must be addressed. While attributes like efficiency and sustainability have been mentioned, the primary goal of this research is not to design more efficient or environmentally friendly processes. Thus, the level of the initial strain value is not as concerning as the manner and degree in which it changes. Since this research assumes systems have been designed to operate safety at their base or initial conditions, the departure from those initial conditions, or range of the system, is of primary concern. This harkens back to the safety description given earlier in Chapter III in the "Energy and Safety" section, where it was stated that systems are designed to withstand a certain load of energy and applied loads outside those bounds might cause failures. By assuming the initial conditions are the beginning of the range, departure from the expected stress-strain behavior can be used as criteria to determine the end of the range for a specific variable.

COMPOSITE SYSTEM CURVES

While the individual variable curves for each system are helpful to seeing how the system behavior changes for different types of stresses, placing all the data on one curve would help with seeing how each type of stress relates to each other type. Thus, Figure 15 shows the steam pipe with all three stresses types (mass flow, temperature, and pressure changes). A detailed legend for Figure 15 is shown in Table 7.

Figure 15: Composite System Curve, Steam Pipe

Table 7: Detailed Legend for Composite Steam Pipe Graph (Figure 15)

Series Number	Mass Flow Value or Range	Temperature Value or Range	Pressure Value or Range
1	$m_f = 8 - 28$ kg/s	$T = 500^oF$	$P = 100$ psia
2	$m_f = 8 - 28$ kg/s	$T = 600^oF$	$P = 100$ psia
3	$m_f = 8 - 32$ kg/s	$T = 700^oF$	$P = 100$ psia
4	$m_f = 8 - 34$ kg/s	$T = 800^oF$	$P = 100$ psia
5	$m_f = 8 - 34$ kg/s	$T = 500^oF$	$P = 150$ psia
6	$m_f = 8 - 44$ kg/s	$T = 500^oF$	$P = 200$ psia
7	$m_f = 8 - 58$ kg/s	$T = 500^oF$	$P = 250$ psia
8	$m_f = 10$ kg/s	$T = 500 - 1200^oF$	$P = 100$ psia
9	$m_f = 10$ kg/s	$T = 500 - 1200^oF$	$P = 150$ psia

The curves for the first four series, each at a different temperature with changing mass flow rate, show that same shape with higher temperature curves shifted to higher strain and higher stress values. Higher stress values are due to the higher energy levels while higher strain values can be attributed to greater heat loss to the atmosphere. The changing mass flow rate curves at higher pressures (Series 5-7) show the same shape as

the curves from Series 1-4, however as the pressure increases, the curves shift to lower stress and strain values due to lower initial energy into the system. The changing temperature curves (Series 8 and 9) show a direct relationship as opposed to the inverse relationship of the earlier series. The stress range displayed by the changing temperature curves is much narrower due to the differences in magnitude of the added energy. The difference between the ranges of Series 8 and 9 is difficult to observe due to the small difference in inlet stress values (only the pressure has changed).

The composite curve for the water pipe is shown below in Figure 16 with the detailed legend (Table 8) giving specific values for each variable.
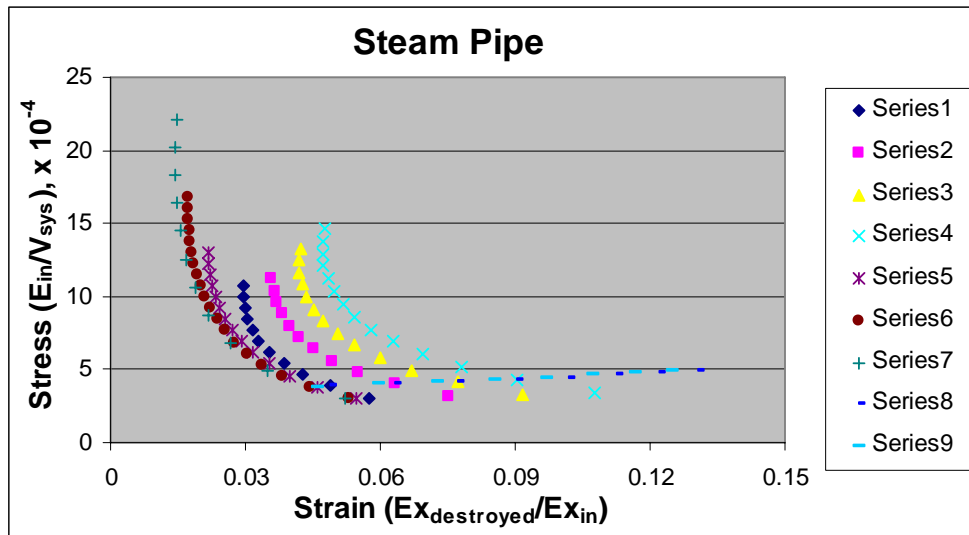

Figure 16: Composite System Curve, Water Pipe

Table 8: Detailed Legend for Composite Water Pipe Graph (Figure 16)

Series Number	Mass Flow Value or Range	Temperature Value or Range	Pressure Value or Range
1	$m_f = 15 - 60$ kg/s	$T = 100^o$F	$P = 50$ psia
2	$m_f = 15 - 100$ kg/s	$T = 150^o$F	$P = 50$ psia
3	$m_f = 15 - 140$ kg/s	$T = 200^o$F	$P = 50$ psia
4	$m_f = 15 - 140$ kg/s	$T = 250^o$F	$P = 50$ psia
5	$m_f = 15$ kg/s	$T = 100 - 220^o$F	$P = 50$ psia
6	$m_f = 15$ kg/s	$T = 100^o$F	$P = 50 - 600$ psia
7	$m_f = 20$ kg/s	$T = 100^o$F	$P = 50 - 550$ psia
8	$m_f = 25$ kg/s	$T = 100^o$F	$P = 50 - 550$ psia
9	$m_f = 30$ kg/s	$T = 100^o$F	$P = 50 - 550$ psia
10	$m_f = 15$ kg/s	$T = 150 - 270^o$F	$P = 50$ psia
11	$m_f = 15$ kg/s	$T = 180 - 280^o$F	$P = 50$ psia

The mass flow rate curves for the water pipe again show the same trends observed for the steam pipe composite curve – as the initial temperature is increased, the mass flow curves shift to higher stress and strain values. However, the lowest temperature curve (Series 1, $T = 100^o$F) displays the inflection point explained in the individual curve section (the strain reaches a minimum before increasing again) while the higher temperature curves decrease, but do not reach a minimum strain). The changing temperature curves (Series 5, 10, and 11) display a very narrow stress and strain range and show an inflection point where the strain reaches a maximum value. The changing pressure curves display a low slope (compared to other series, they appear close to horizontal) with higher mass flow rates curves starting at higher stress values. The small stress ranges of the changing pressure curves is due to the fact that pressure changes cause very small changes in the energy of process streams as compared with mass flow or even temperature changes.

The composite curve for the water pump is shown below in Figure 17) with temperature and mass flow rate changes both displayed. The detailed legend is also given in Table 9
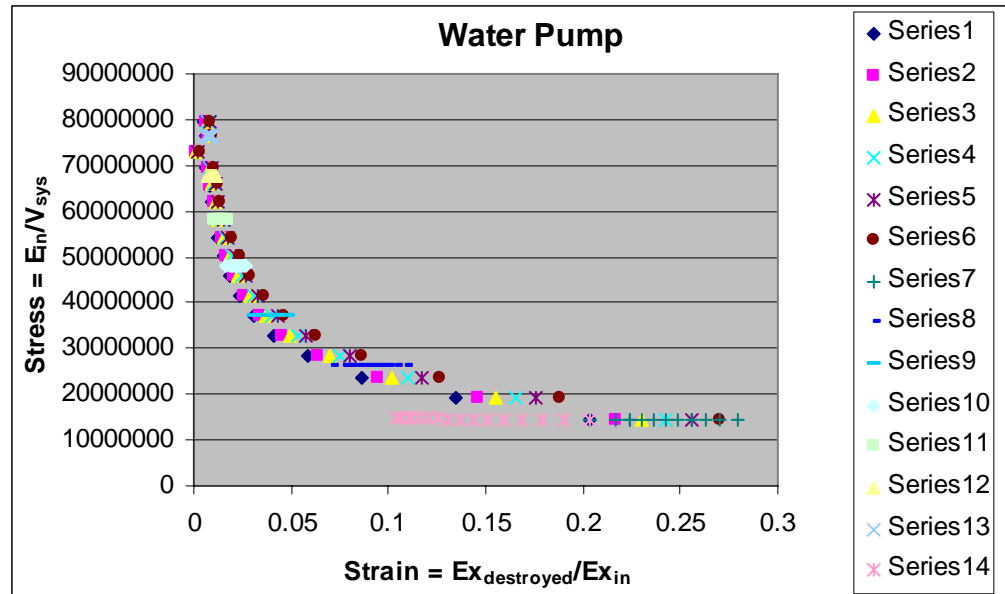
Water Pump
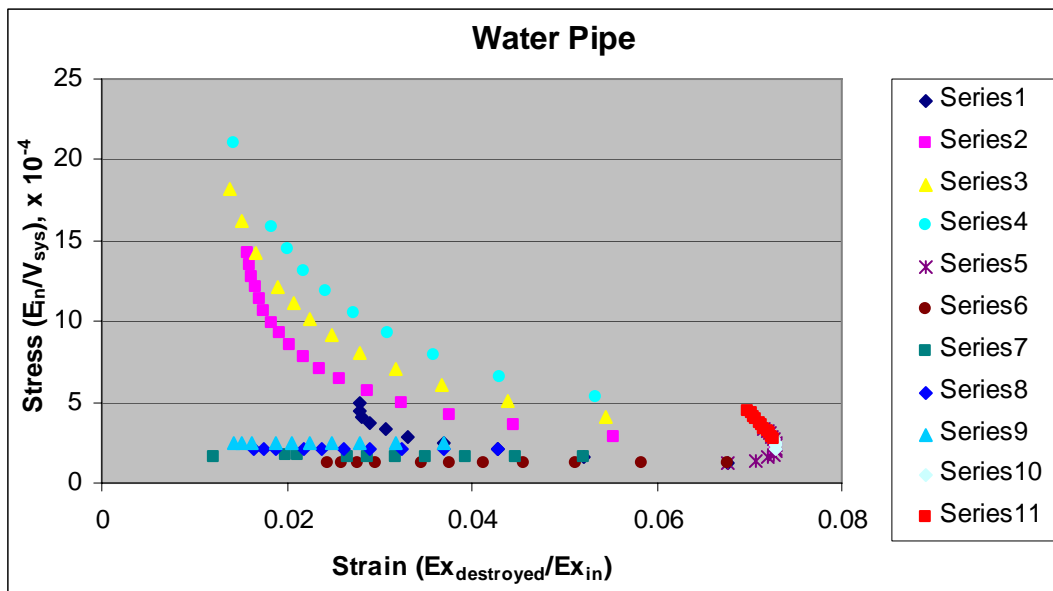
Figure 17: Composite System Curve, Water Pump

Table 9: Detailed Legend for Composite Water Pipe Graph (Figure 17)

Series Number	Volumetric Flow Value or Range	Temperature Value or Range	Inlet Pressure Value or Range
1	$v_m = 750$ gpm	$T = 90 - 410^o$F	$P_{in} = 300$ psia
2	$v_m = 650$ gpm	$T = 90 - 410^o$F	$P_{in} = 300$ psia
3	$v_m = 550$ gpm	$T = 90 - 410^o$F	$P_{in} = 300$ psia
4	$v_m = 450$ gpm	$T = 90 - 410^o$F	$P_{in} = 300$ psia
5	$v_m = 350$ gpm	$T = 90 - 410^o$F	$P_{in} = 300$ psia
6	$v_m = 250$ gpm	$T = 90 - 410^o$F	$P_{in} = 300$ psia
7	$v_m = 750 - 200$ gpm	$T = 90^o$F	$P_{in} = 300$ psia
8	$v_m = 750 - 200$ gpm	$T = 140^o$F	$P_{in} = 300$ psia
9	$v_m = 750 - 200$ gpm	$T = 190^o$F	$P_{in} = 300$ psia
10	$v_m = 750 - 200$ gpm	$T = 240^o$F	$P_{in} = 300$ psia
11	$v_m = 750 - 200$ gpm	$T = 290^o$F	$P_{in} = 300$ psia
12	$v_m = 750 - 200$ gpm	$T = 340^o$F	$P_{in} = 300$ psia
13	$v_m = 750 - 200$ gpm	$T = 390^o$F	$P_{in} = 300$ psia
14	$v_m = 750$ gpm	$T = 90^o$F	$P_{in} = 300 - 1000$ psia

All the changing temperature curves (Series 1-6) show very similar shape with the lower volumetric flow curves shifting to slightly higher strain values. However, the curves remain at very similar stress values due to the manner in which pump volume was defined (see pump individual curve section). The changing volumetric flow rate curves (Series 7-13) again appear close to horizontal with higher temperature curves positioned at higher stress and lower strain values. The flow rate curves correspond well with the temperature curves – they generally seem to range over strain values covered by the temperature curves at that stress level. The changing inlet pressure curve (Series 14) is positioned at approximately the same stress level as the same temperature changing flow rate curve (Series 7), however the pressure curve has a very slightly downward slope and ranges over lower strain values.

The heat exchanger composite graph (Figure 18) and detailed legend (Table 10) are shown below. There are fewer variations shown on the graph due to the difficultly of obtaining data – a great deal of iterating was required for each series of data, thus limited variations were performed.
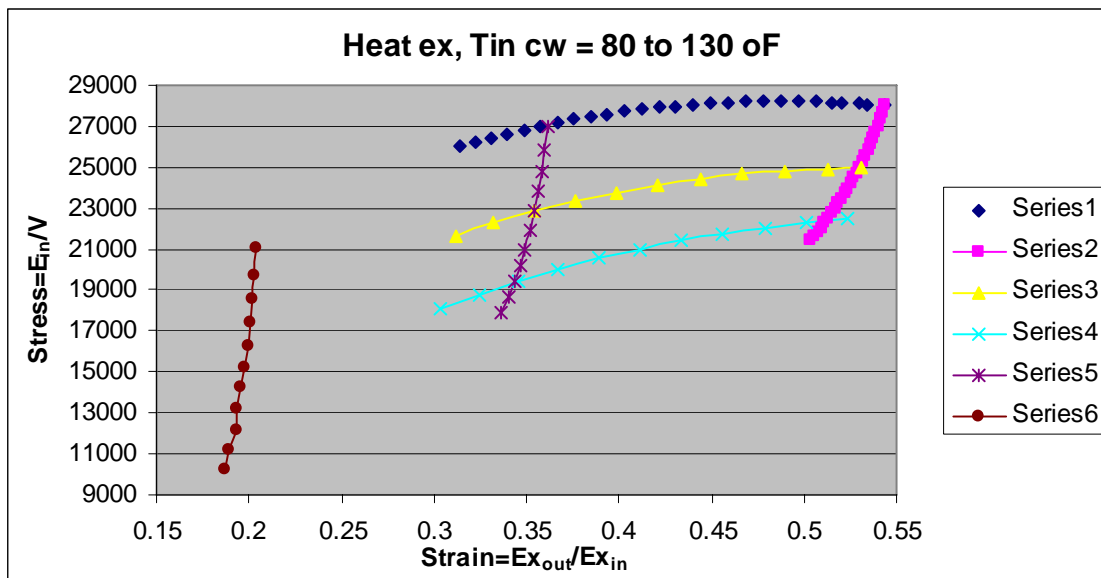
Figure 18: Composite System Curve, Heat Exchanger

Table 10: Detailed Legend for Composite Heat Exchanger Graph (Figure 18)

Series Number	Inlet Cooling Water Temperature	Inlet Steam Mass Flow Rate
1	$T = 80 - 130^{\circ}F$	$m_f = 50$ kg/s
2	$T = 80^{\circ}F$	$m_f = 50 - 75$ kg/s
3	$T = 80 - 130^{\circ}F$	$m_f = 60$ kg/s
4	$T = 80 - 130^{\circ}F$	$m_f = 70$ kg/s
5	$T = 120^{\circ}F$	$m_f = 50 - 75$ kg/s
6	$T = 160^{\circ}F$	$m_f = 50 - 80$ kg/s

The heat exchanger curves display distinctly different shapes for the different system changes – the changing temperature curves (Series 1, 3, 4) begin at lower stress values and slightly lower strain values as the inlet steam mass flow rate increases. The lower stress value are due to the higher volume while the lower strain values can be attributed to the higher initial amount of exergy within the system (smaller percent exergy transferred). The changing mass flow rate curves display a steeper slope as they move from higher to lower strain values. The curves begin at significantly lower stress and strain values as the temperature increases. Again, the lower stress and strain values can be attributed to higher volumes and higher initial exergy values. However, the curves do appear to vary within a common area – the upper and lower points of the changing temperature curves fall near or on the changing mass flow rate curves (the lowest point falls slightly under the lowest changing temperature curve, but this is due that curve being run at 70 kg/s as opposed to the maximum 75 kg/s flow rate seen in the mass flow rate variations.)

SUMMARY

This chapter presented preliminary characteristic system curves for the steam pipe, water pipe, water pump, and heat exchanger systems. Curves for all "stresses," or variables changes were presented for each system. The trends and significance of the curves were examined on a qualitative basis and discussed. Curves were also presented which showed all stress for each system on the same graph.

Currently, all the work for this research has focused on qualitative assessments of resilience. Graph shapes and trends have been examined but no quantitative comparisons have been attempted. The next chapter will show the development of a quantitative method that will allow resilience to be compared both for different stresses to the same system and also for comparison of different system designs.

CHAPTER VI

QUANTIFICATION

While the last chapter showed how each system behaved qualitatively over a range of variables, it would be desirable to develop quantitative measures or methods by which these graphs and systems could be compared and contrasted. Now that characteristic system curves has been created, it would be helpful to identify the point on the curve that shows departure from resilience and thus the region within which the system exhibits resilient behavior.

RESILIENT REGION DETERMINATION

For materials that are linearly elastic, the resilient region can be seen as the section of the graph displaying a linear slope – there is a direct, linear relationship between material stress and material strain.[54] However, not all materials are linear elastic and display a linear relationship in the resilient region. Different types of materials are characterized by different relationships between stress and strain, even within the resilient region. By the same reasoning, systems will also display a variety of behavior types within their resilient regions. Therefore, characterizing the resilient behavior of systems will not simply involve identifying a linear slope region and then determining when deviations occur. The behavior of the resilient regime will differ not only for different systems, but also for different starting points to the same system.

It would be useful if the functional relationship between system stress and system strain could be determined. Thus, the point at which the system deviated from the established functional relationship could be determined and the resilient regime could be set as the period where the system behaves as predicted by the established function. However, as seen in the characteristic system curves from the previous chapter, the curve trends vary greatly, but with the exception of the few inflection points, the curves tend to trend either upwards or downwards with a slope that is either consistently

decreasing or consistently increasing (i.e. the slope does not increase then decrease or vise versa).

Thus, a power-law trend-line was chosen to fit the data due to its flexibility of fit. An equation for a power-law trend-line is given below where A and B are correlation parameters determined from the data.

$$Sn = A(Ss)^B \tag{6.1}$$

Where:

$A =$ correlation factor

$B =$ exponent of fit

Power law trend-lines are attractive because they provide accurate relationships for linear data ($B=1$), directly related data with an increasing slope trend ($B>1$), and inversely related data with a decreasing slope trend (negative B). Figure 19 below shows some of the behavior of these curves. As can be seen, the A value was assumed to be one for these examples and each curve shows x-values from 0.1 to 0.6 (close to common strain values). The negative B example ($B=-0.1$) shows an inverse relationship between x and y while the $B=1$ case shows a straight line with a slope of B. The $B=0.2$ case shows a direct relationship between stress and strain, however the curve shows a decreasing slope trend.
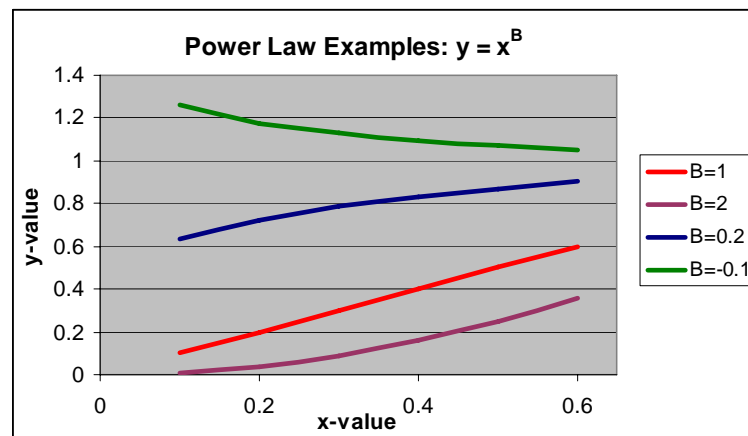
Figure 19: Example of Behavior of Different Power Law Equations

Significant Uses of Power Laws

There is precedent to using power law relationships to predict system behavior from complex system analysis. Power laws have been observed to describe the statistics of events for interconnected systems such as the probability of a certain size forest fire and the distribution of file download sizes.[29] Similar relationships have also been observed for data sets relating to species extinctions, traffic jams, and the volatility of financial markets.[29] The research framework of highly optimized tolerance (HOT) claims these power law observations demonstrate a link between internal structure and power law behavior.[55] The HOT framework attempts to understand complex system behavior by emphasizing that biological and engineered systems are highly structured systems which display robust yet fragile external behavior (robust to numerous random failures, fragile in that failure of certain critical components could be catastrophic.)

While the presence of power law relationships could be unrelated to the goal of predicting safe and unsafe system behavior, the fact that power laws have been observed in varied systems ranging from biology to machinery seems to indicate this behavior is not necessarily just a reflection of internal system structure – if it were strictly system specific, significantly different behavior would be expected for systems composed of different components. Thus, it is reasonable to assume that these power laws can be used to predict critical phenomena exhibited by many-component, complex systems.[55]

Power law behavior can also be observed within the realm of fluid dynamics. For soft solids and structured liquids, low stress creep behavior can often be described as Newtonian. However, flow behavior transitions to a power-law relationship between shear stress and steady-state shear rate at higher stress values.[56] Since all system presented are under a significant amount of stress (none of the systems begin at the zero stress point and then increase the stress) and all the systems involve material flows, the assumption of a power law relationship for the behavior of these test systems may be reasonable. While this power law relationship is being used for stress versus strain as opposed to stress versus shear rate,[56] time is represented in the system stress variable

(units of energy per volume per unit time) due to the presence of an energy flow rate within each test system.

Power Law Application

For the region of the system stress-strain curve that follows the power-law relationship, the use of a best-fit line will introduce little error – i.e. the R^2 value, or coefficient of determination, of the power trend-line will be close to one. However, if the R^2 value of the trend-line begins to decrease, this indicates some deviation of the data from the expected functional relationship. Thus, the decline of the R^2 value will be used to determine the yield point and subsequent end of the resilient region. The resilient region will be assumed to be the region where the R^2 value is equal to or higher than 0.99.

The point at which the curve deviates from the expect trend will vary for different systems, different stress types, and different stress levels. It is assumed that the system has been properly designed to withstand the stress and strain the system is initially under (the point where the curve begins). Thus, the resilient region measures how large of a stress or strain range the system can operate within while still displaying a power law relationship between stress and strain that describes data within the entire operating region. This will vary because depending on the initial stress and strain; the system may be able to withstand larger or smaller deviations. For example, a system designed to withstand a higher temperature (if volume is constant, this will result in a higher initial stress) may be able to withstand larger energy fluctuations or may have more avenues available by which the system can dissipate additional energy loads. Of course, the opposite may be true – a system under higher stress may be limited to withstanding a smaller range due to the fact that the normal operating energy level consumes much of the system's available energy capacity.

Resilience can be characterized by the determination of regions with predictable or expected behavior due in part to the precedent from material science (resilience characterized by a predicable, linear slope) as well as considerations from process

control. Many control systems require system properties to be predicted by a process model – if behavior stays within what can be modeled and predicted by a mathematical function, the system may be more likely to remain operable and controllable under changing conditions. Also, from the perspective of system knowledge, if the system behavior remains predictable, the operator's ability to understand how the system will act with different variable changes will be greater.

CURVE FIT PROCEDURE

While Excel will fit trend-lines through graphical data and display curve equations and R^2 values, since the R^2 value and curve equation were desired for the curve every time a subsequent point was added to the range, the use of this feature would be unfeasible. Curve fitting was performed using the series of stress and strain values with the strain value being the x-coordinate and the stress value corresponding to the y-coordinate.

Power-law regression was performed using the same equations used for linear regression after the power-law equation was transformed as shown below:

$$\ln y = \ln(Ax^B) = \ln A + \ln(x^B) = \ln A + B\ln x \tag{6.2}$$

The equation for the slope (b) of a simple, linear, least-squares regression line was calculated as:[57]

$$b = \frac{n\sum xy - (\sum x)(\sum y)}{n\sum x^2 - (\sum x)^2} \tag{6.3}$$

Where:

$n =$ number of data points

$x =$ system strain

$y =$ system stress

Thus, the power law B correlation coefficient was calculated by substituting the natural logs of x and y, resulting in the following equation:

$$B = \frac{n\sum_{i=1}^{n}(\ln x_i \times \ln y_i) - \sum_{i=1}^{n}\ln x_i \sum_{i=1}^{n}\ln y_i}{n\sum_{i=1}^{n}(\ln x_i)^2 - (\sum_{i=1}^{n}\ln x_i)^2}$$ (6.4)

The intercept, a, for a simple, linear, least-squares regression line was calculated from[57]

$$a = \frac{\sum y - b \sum x}{n}$$ (6.5)

Thus, since the intercept of the transformed line equals the natural log of A, the intercept equation was transformed and used to determine A as follows:

$$A = \exp\left(\frac{\sum_{i=1}^{n}\ln y_i - B\sum_{i=1}^{n}\ln x_i}{n}\right)$$ (6.6)

The trend-line equation that best fits the range of data as each subsequent point was added was now known. An estimated stress value was then determined from this equation as shown below:

$$\hat{y} = Ax^B$$ (6.7)

Where:

$\hat{y} =$ estimated system stress value from best fit data and corresponding system strain value

Now, this estimated system stress value was used to calculation the sum of squared errors, SSE_n, for the fit.[57]

$$SSE_n = \sum_{i=1}^{n}\left[\ln y_i - \ln \hat{y}_i\right]^2$$ (6.8)

The total sum of squares, SST_n, was determined from:[57]

$$SST_n = \sum_{i=1}^{n}\left(\ln y_i - \frac{\sum_{i=1}^{n}y_i}{n}\right)$$ (6.9)

With these two sums, the R^2 value for the fit was determined using the following equation:[57]

$$R^2 = \frac{SST_n - SSE_n}{SST_n}$$
(6.10)

CURVE FIT RESULTS

Curves were fit to the data sets for each of the case studies. Data from the steam pipe test case are shown in Table 11 below. The table shows the $A, B,$ and R^2 values for the changing mass flow rate curve where the temperature was held constant at 500°F and the pressure was set at 100 psia (curve number 1 from the composite steam test case graph shown in Figure 15.)

Table 11: Curve Fit Data for the Steam Pipe Case, T = 500°F and P = 100 psia

Mass Flow Rate (kg/s)	System Stress	System Strain	A	B	R^2
8	3.083E+04	0.05762			
10	3.853E+04	0.04883	657.8	-1.348	1.000
12	4.624E+04	0.04276	638.0	-1.359	1.000
14	5.395E+04	0.03843	601.3	-1.379	0.9999
16	6.165E+04	0.03531	551.1	-1.408	0.9995
18	6.936E+04	0.03306	491.2	-1.446	0.9985
20	7.707E+04	0.03149	425.9	-1.493	0.9965
22	8.477E+04	0.03045	359.1	-1.548	0.9927
24	9.248E+04	0.02986	294.9	-1.612	0.9862
26	1.002E+05	0.02964	236.5	-1.684	0.9758
28	1.079E+05	0.02975	186.3	-1.761	0.9597

There is no value for $A, B,$ or R^2 in the first row ($m_f = 8$ kg/s) since at least two points were required for curve fitting. As can be seen from the chart, the R^2 value fell below 0.99 after the mass flow rate was increased above 22 kg/s. It should also be noted that

while the coefficient of determination decreases slowly in the range of m_f = 8 to 22 kg/s, after the R^2 value drops below 0.99, it begins to decrease rapidly indicating the data begins to deviate significantly from the previously-established power-law relationship. As described in the previous chapter for the individual steam pipe changing mass flow rate curve, as the mass flow rate increases, the proportional amount of exergy destroyed decreases due to the leveling off of the friction factor. While this immediate cause contributes to the deviations from the power-law behavior, it should be noted that the resilient region ends well before the limiting condition of the onset of sonic flow.

While these data are informative, it would be more informative to observe how the resilient region changes with different system stress types. Thus, Table 15 shows the points just above and just below R^2 = 0.99 for each of the curves on the composite steam pipe graph shown in Figure 15. The conditions for each curve (temperature, pressure, and mass flow rate are also given.)

Some trends can be identified from the data shown in Table 12. As the temperature of the process is increased, the allowable mass flow rate range also increases. One possibility for this is that higher temperature systems have been designed to withstand a larger base energy load and thus can tolerate larger energy fluctuations. Another point to note is that one limiting condition, the onset of sonic flow, depends on the temperature of the fluid: higher temperature result in higher velocities (and thus higher mass flow rates) for sonic flow. Also, equal increment fluctuations cause a smaller percentage change in the applied energy load for systems designed for higher initial loads. While there are not a great deal of data present for the changing pressure case, the two curves shown seem to indicate that the allowable temperature range is not very dependent on the initial pressure as the allowable temperature range does not change when the initial system pressure is increased from 100 psia to 150 psia. One possible reason for this is that increasing the pressure within a system does not cause as large of a change in the energy of the process stream as the change caused by changing temperature or mass flow rate.

Table 12: Curve Fit Data for the Steam Pipe Test Case

Curve #	m_f (kg/s) value / range	T (°F) value / range	P (psia) value / range	System Stress, x 10^{-4}	System Strain	A	B	R^2
1	8 - 22	500	100	8.477	0.03045	359.1	-1.548	0.9927
	8 - 24	500	100	9.248	0.02986	294.9	-1.612	0.9862
2	8 - 20	600	100	8.009	0.03968	794.9	-1.421	0.9980
	8 - 22	600	100	8.810	0.04060	622.3	-1.509	0.9790
3	8 - 26	700	100	10.80	0.04263	904.6	-1.491	0.9905
	8 - 28	700	100	11.63	0.04209	789.3	-1.542	0.9840
4	8 - 26	800	100	11.20	0.04831	1346	-1.437	0.9931
	8 - 28	800	100	12.06	0.04746	1205	-1.481	0.9883
5	8 - 30	500	150	11.51	0.02211	471.9	-1.422	0.9930
	8 - 32	500	150	12.28	0.02178	421.6	-1.457	0.9891
6	8 - 38	500	200	14.53	0.01754	531.6	-1.364	0.9926
	8 - 40	500	200	15.29	0.01735	490.2	-1.388	0.9896
7	8 - 43	500	250	16.37	0.01489	625.3	-1.305	0.9950
	8 - 48	500	250	18.27	0.01452	542.6	-1.346	0.9896
8	10	500 - 900	100	4.460	0.1021	6.915 E+04	0.1960	0.9901
	10	500 - 1000	100	4.616	0.1127	7.245 E+04	0.2128	0.9841
9	10	500 - 900	150	4.455	0.09686	7.004 E+04	0.1973	0.9914
	10	500 - 1000	150	4.611	0.1073	7.329 E+04	0.2134	0.9859

Curve fit data are shown below in Table 13 for the base case, changing mass flow rate for the water pipe test system. The temperature was held constant at 100°F while the pressure was set at 50 psia. The mass flow rate was changed in 5 kg/s increments from a starting flow rate of 15 kg/s.

Table 13: Curve Fit Data for the Water Pipe Case, T = 100°F and P = 50 psia

Mass Flow Rate (kg/s)	System Stress, x 10^{-4}	System Strain	A	B	R^2
15	1.232	0.06776			
20	1.643	0.05206	653.2	-1.091	1.000
25	2.053	0.04282	616.7	-1.112	0.9999
30	2.464	0.03697	569.8	-1.140	0.9996
35	2.875	0.03313	514.6	-1.175	0.9987
40	3.285	0.03061	453.7	-1.218	0.9966
45	3.696	0.02904	390.5	-1.269	0.9926
50	4.106	0.02817	328.5	-1.326	0.9855
55	4.517	0.02786	270.9	-1.391	0.9740
60	4.928	0.02800	220.3	-1.460	0.9561

The R^2 value falls below 0.99 as the mass flow rate is increased above 45 kg/s. Again, the R^2 value decreases slowly as the flow rate is changed from 15 to 45 kg/s, but decreases relatively rapidly after the R^2 value decreases below 0.99. Again, the proportional amount of exergy dissipated decreases as the velocity increases with the increasing mass flow rates. One important note about the water pipe results is the extremely small strain values. While the resilient ranges capture the region where the system's response is predictable by a power-law trend, the ranges do not hold as much meaning for this case due to how small the strain values are. Water pipes operation extremely close to ideality (very small strains), so even large percentage departures result in small strain values and small absolute changes in exergy values. Table 14 below summarizes the curve fit data for different curves and variable changes applied to the water pipe system.

Table 14: Curve (Cv) Fit Data for the Water Pipe Test Case

Cv #	m_f (kg/s) value / range	T (°F) val. / rnge	P (psia) value / range	System Stress, x 10^{-4}	System Strain	A	B	R^2
1	15-45	100	50	3.696	0.02904	390.5	-1.269	.9926
	15-50	100	50	4.106	0.02817	328.5	-1.326	.9855
2	15-90	150	50	12.80	0.01625	943.3	-1.167	.9925
	15-95	150	50	13.52	0.01602	887.2	-1.186	.9898
3	15-130	200	50	26.34	0.01156	1403	-1.143	.9925
	15-140	200	50	28.37	0.01143	1297	-1.166	.9890
4	15-140	250	50	R^2 stays above 0.99 for entire observed range				
5	15	100-110	50	1.412	0.07069	7.407E+7	3.233	1.000
	15	100-120	50	1.593	0.07201	6.738E+8	4.056	.9832
6	15	100	50-450	1.251	0.02964	1.171E+4	-.01842	.9901
	15	100	50-500	1.253	0.02770	1.168E+4	-.01937	.9886
7	20	100	50-350	1.662	0.02650	1.561E+4	-.01710	.9940
	20	100	50-400	1.668	0.01207	1.593E+4	-.01088	.9707
8	25	100	50-450	2.085	0.01873	1.936E+4	-.01842	.9901
	25	100	50-500	2.089	0.01750	1.930E+4	-.01937	.9886
9	30	100	50-450	2.502	0.01617	2.317E+4	-.01842	.9901
	30	100	50-500	2.507	0.01511	2.309E+4	-.01937	.9886
10	15	150-170	50	2.496	0.07277	5.137E-65	-60.36	.9944
	15	150-180	50	2.677	0.07260	9.654E-46	-43.41	.9881
11	15	180-280	50	R^2 stays above 0.99 for entire observed range				

The identifiable trends from these data include that again the allowable mass flow rate increases as the initial temperature of water is increased. The allowable pressure range stays constant as the mass flow rate increases with the exception of the 20 kg/s initial flow rate case. The cases involving changing temperature (curves 5, 6, and 9-11) display unusual results – the allowable range is quite small (10 to 20 degrees) for cases where the initial temperature is 100°F – this is most likely due to the presence of an inflection point in the curve as observed in Figure 16 in the chapter "Results and Analysis." The changing temperature curve reaches a maximum strain point at a temperature of 150°F. Thus, the behavior of the curve changes significantly around this point and as expected, trend-lines are only sufficient to predict system behavior for small ranges (as seen for curves 5,6, 9, and 10). As the starting temperature is moved away from the inflection point (curve 11), the power law trend can again be used to predict a wide variable range (temperature ranging from 180 to 280°F). Again, it should be kept in mind that due to extremely small strain values, small fluctuations in system or material properties could cause noticeable changes in the allowable ranges.

Table 15 below summarizes allowable ranges for the water pump system.

Table 15: Curve Fit Data for the Water Pump Test Case

Curve #	Vol Flow Rate (gpm)	Water P_{in}, psia	Water T_{in}, °F	System Stress, x 10^{-7}	System Strain	A, x 10^{-6}	B	R^2
1	750	20.68	90-350	6.937	0.006506	7.748	-0.4440	0.9967
	750	20.68	90-370	7.289	0.000916	10.93	-0.3400	0.9206
2	650	20.68	90-350	6.939	0.007201	7.982	-0.4475	0.9963
	650	20.68	90-370	7.291	0.001162	10.93	-0.3496	0.9253
3	550	20.68	90-350	6.941	0.007875	8.198	-0.4506	0.9960
	550	20.68	90-370	7.293	0.001444	10.91	-0.3589	0.9301
4	450	20.68	90-350	6.943	0.008544	8.407	-0.4533	0.9956
	450	20.68	90-370	7.295	0.001778	10.88	-0.3681	0.9352
5	350	20.68	90-350	6.944	0.009238	8.623	-0.4557	0.9953
	350	20.68	90-370	7.296	0.002187	10.86	-0.3775	0.9408
6	250	20.68	90-350	6.946	0.01003	8.868	-0.4580	0.9949
	250	20.68	90-370	7.298	0.002731	10.84	-0.3877	0.9472
7	200-750	20.68	90	R^2 stays above 0.99 for entire observed range				
8	200-750	20.68	140	R^2 stays above 0.99 for entire observed range				
9	200-750	20.68	190	R^2 stays above 0.99 for entire observed range				
10	200-750	20.68	240	R^2 stays above 0.99 for entire observed range				
11	200-750	20.68	290	R^2 stays above 0.99 for entire observed range				
12	200-750	20.68	340	R^2 stays above 0.99 for entire observed range				
13	200-750	20.68	390	R^2 stays above 0.99 for entire observed range				
14	750	20.7-68.9	90	R^2 stays above 0.99 for entire observed range				

The water pump data show remarkable agreement for the allowable temperature ranges. For every flow rate curve, the allowable temperature range remained 90 to 340°F. As the temperature increases above 340°F, pump cavitation quickly onsets, so this range does limit operation to ending prior to a known point of concern. One reason for the remarkable agreement of the ranges is the manner in which the volume of the pump was calculated – since the volume of the pump was determined by dividing the volumetric flow rate by the specific speed (in revolutions per minute) – this determined the volume inside the pump available for fluid at any moment. Thus, the volume factors into both the energy term (via the material stream) in the numerator and in the

denominator (volume of the system). For the other variable ranges investigated, the R^2 value did not drop below 0.99 during the range. One reason for this in the changing volumetric flow rate case is again the presence of the volumetric flow rate both the numerator and denominator of the stress variable as well as the fact that the pumps was designed to operate anywhere from 100 gallons per minute (gpm) to approximately 1500 gpm.

The results from the heat exchanger curves are shown below in Table 16.

Table 16: Curve Fit Data for the Heat Exchanger Test Case, Inlet Water P=100 psi, Inlet Water m_f=674 kg/s, Inlet Steam P=50 psi

Curve #	Water T_{in}, °F	Steam m_f, kg/s	System Stress x 10^{-3}	System Strain	A, x 10^{-4}	B	R^2
1	80-86	50	28.17	0.5156	2.626	-0.1060	0.9938
	80-88	50	28.20	0.5062	2.647	-0.09340	0.9844
2	80	50-75	R^2 stays above 0.99 for entire observed range				
3	80-95	60	24.66	0.4667	2.667	0.1016	0.9902
	80-100	60	24.43	0.4438	2.710	0.1255	0.9833
4	80-110	70	20.54	0.3891	2.747	0.3026	0.9908
	80-115	70	20.01	0.3672	2.797	0.3266	0.9891
5	120	50-65	20.98	0.3493	4293	7.259	0.9919
	120	50-67.5	20.24	0.3464	2464	6.718	0.9892
6	160	50-62.5	15.24	0.1978	6.631E+07	10.86	0.9912
	160	50-65	14.22	0.1958	1.239E+07	9.815	0.9890

Observable trends include that the allowable cooling water temperature range increases as the steam mass flow rate increases. This is somewhat counter-intuitive and is partially be due to the fact that the calculations allowed the exchanger length to vary as the inlet parameters were changed. The higher steam flow exchangers required longer lengths, thus the volume of the exchanger was higher. As the inlet water temperature increased, the allowable steam mass flow rate range decreased. This is expected, as the

thermal driving force of the exchanger decreased when the inlet water temperature increases, thus leaving less capacity for the water stream to remove heat from the steam stream.

Allowing the length to change with variable changes is not necessarily realistic in helping to understand the affect of different variables on allowable ranges, since each different variable change results in a different exchanger. Thus, the affects of variable changes on allowable resilient ranges will be explored in more detail in the next chapter as the same heat exchanger is simulated for different conditions.

SUMMARY

A quantifiable method for determining resilient ranges for systems was developed and presented. Power law relationships, which have be used to describe a variety of different type of system properties, were fit to data to describe the functional relation between system stress and strain. The methodology was then applied to each of the four test systems to determine how different stresses affected the allowable resilient ranges.

CHAPTER VII
COMBINED SYSTEM SIMULATION

The last chapter outlined the quantification method chosen to determine resilient ranges for different systems. However, due to calculation limitations, only limited results from individuals system were shown. Also, while the method was shown to work for individual systems, it is critical that the method show scalability, i.e. the method work for large systems consisting of multiple, connected individual process components.

Therefore, the process simulator ASPEN was used to generate results for alarger, combined systems as well as the four individual equipment components.

SIMULATOR INPUT SETTINGS

The overall system was formed by combining the four individual systems: water pipe, steam pipe, water pump, and steam condenser. The equipment was linked by allowing the water stream to flow through the water pipe, then into the water pump, and finally through the tube side of the condenser. The steam flowed through the steam pipe and then into the shell side of the condenser. The process layout is shown below in Figure 20.
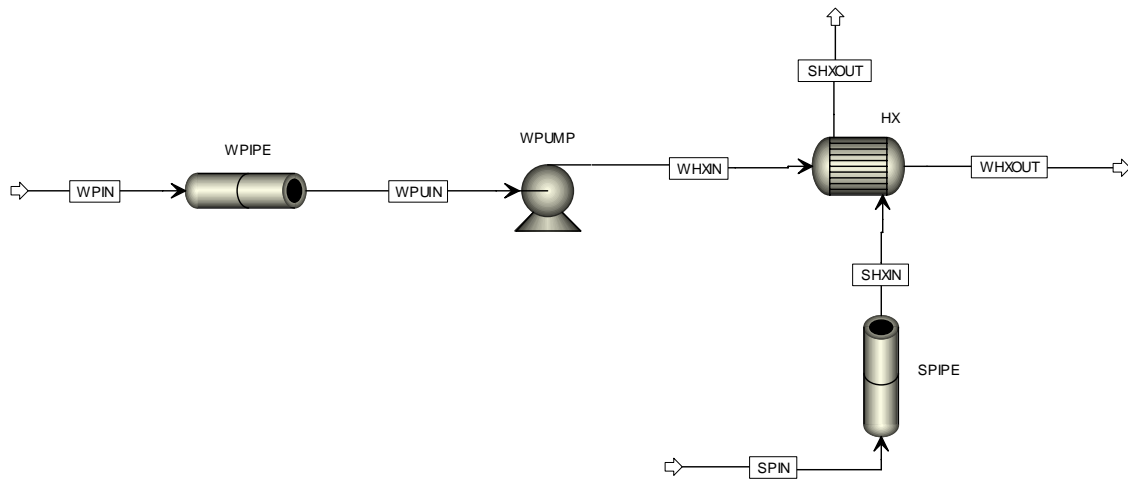
Figure 20: Process Layout for Combined System

A general simulation was conducted in ASPEN with property type "steam-ta" indicating the ASME (American Society of Mechanical Engineers) Steam Tables were used for properties. The steam pipe was a 50-foot carbon steal pipe with roughness of light rust, schedule 40 thickness, no fittings, and flanged and welded connections. A 36-inch diameter was chosen to ensure the velocity was sufficiently under sonic conditions while still ensuring fully developed turbulent conditions existed. The pipe was surrounded by a 70°F atmosphere.

The water pipe was similarly a 50-foot carbon steel pipe with no fittings, light rust roughness, schedule 40 thickness, and flanged and welded connections. An 18-inch pipe was chosen to ensure velocity was sufficiently under sonic conditions while ensuring fully developed turbulent flow occurred. The pipe was again allowed to exchange heat with a 70°F atmosphere. The water pump was set to operate with an efficiency of liquid compression of 0.80 and a motor efficiency of 0.65. The pump was set to impart a constant 300-psi increase to the water stream.

The exchanger used was a TEMA (Tubular Exchangers Manufacturer's Association) shell type E countercurrent horizontal steam condenser, with one shell and

one tube pass. The 12.75 meter long exchanger was chosen to have an shell inside diameter of 37 inches and the exchanger contained 674 bare, one-inch nominal diameter carbon steal tubes. The tubes were situated at a 1.25-inch triangular pitch with a 16 BWG (Birmingham Wire Gauge) thickness. As per ASPEN minimum requirements, the exchanger was assumed to have two segmented baffles with tubes in the baffle window. The inlet nozzles were set at the same diameter of the water and steam pipes. The outlet diameter of the tube side was set equal to the inlet diameter while the outlet shell side diameter was sized to prevent large velocity changes for the steam stream.

The initial conditions of the water stream into the water pipe were set at 100°F, 50 psia, and 674 kg/s (1 kg/s per tube in the exchanger). The conditions of the steam into the water pipe were set as 500°F, 100 psia, and 30 kg/s. The "stresses" applied to the system allowed the water temperature to vary from 100 to 280°F, the water pressure to change from 50 psia to 750 psia, and the water mass flow rate to vary from 674 to 1174 kg/s. The steam conditions were varied from 500°F to 1200°F, from 100 psia to 280 psia, and from 30 kg/s to 55 kg/s. The water pipe, water pump, and heat exchanger were affected by changes to the water stream and the steam pipe and heat exchanger were affect by steam stream changes. The water pump and pipe were unaffected by changes in the steam stream while the steam pipe was unaffected by water stream changes.

SIMULATOR RESULTS

The simulations provided property information for all inlet and outlet streams. From these conditions, stress and strain variables were calculated both for each individual piece of equipment as well as the overall system.

Individual System Results

Characteristic system curves as well as variable ranges were determined for all four individual components. The steam pipe overall system curve is shown below in Figure 21. As can be seen, the trends for each of the curves are similar to those trends established for the steam pipe hand calculations in Figures 5 through 7. The mass flow

rate curve shows an inverse relationship while the temperature curve displays a direct relationship between system stress and strain. The changing pressure curve shows a direct relationship, however the stress range covered by the pressure curve is extremely small compared to the ranges for the mass flow and temperature curves due to the fact that as the pressure changes, the energy load applied to the pipe does not change a significant amount. Each curve proceeds outward from a common point (representing the base case of 500°F, 100 psia, and 30 kg/s). Again, the range covered by the pressure curve is quite small while the temperature curve varies over a large stress range though only a moderate stain range and the pressure curve range reverses that trend with a large strain range and moderate stress range.
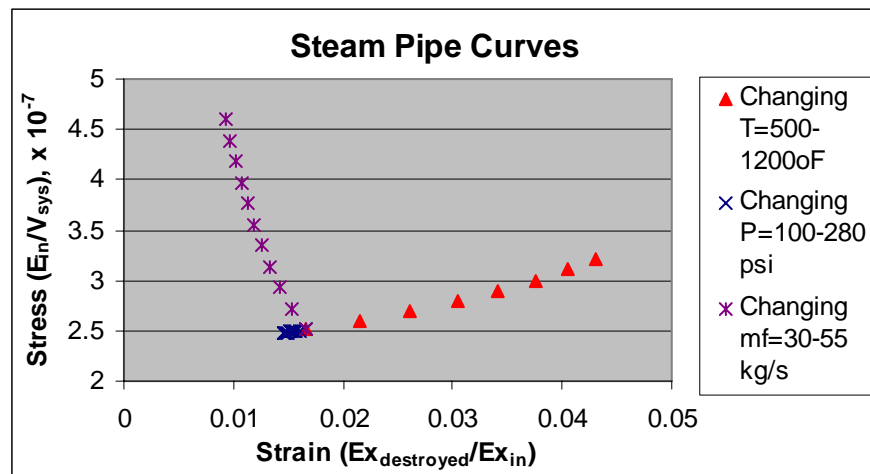
Figure 21: Steam Pipe Results (as part of the Overall System Simulation)

The simulated water pipe curve is shown below in Figure 22. Again, some of the trends exhibited in this curve mirror earlier established trends. The pressure curve shows an inverse relationship with covering a very narrow stress range. The temperature curve shows a direct relationship – the curve in Figure 9 displays both direct and inverse relationships due to the presence of an inflection point around T=150°F. No inflection

point is observed for this temperature curve due to the differences in mass flow rate between this system (m_f=674 kg/s) and the earlier system (m_f=16 kg/s) – the inflection point may be positioned at a different temperature level. The mass flow rate follows a direct relationship as opposed to the inverse relationship shown in Figure 8, however the curve in Figure 8 appeared to have reached an inflection point at the end of the mass flow rate range (m_f=15 to 60 kg/s) due to the fact that the strain values reached a minimum at m_f=55 kg/s. Since this mass flow rate range is significantly higher than the earlier investigated range, it seems probable that like the temperature curve behavior, the mass flow rate curve displays a behavior change at the inflection point with behavior switching from an inverse to a direct relationship.
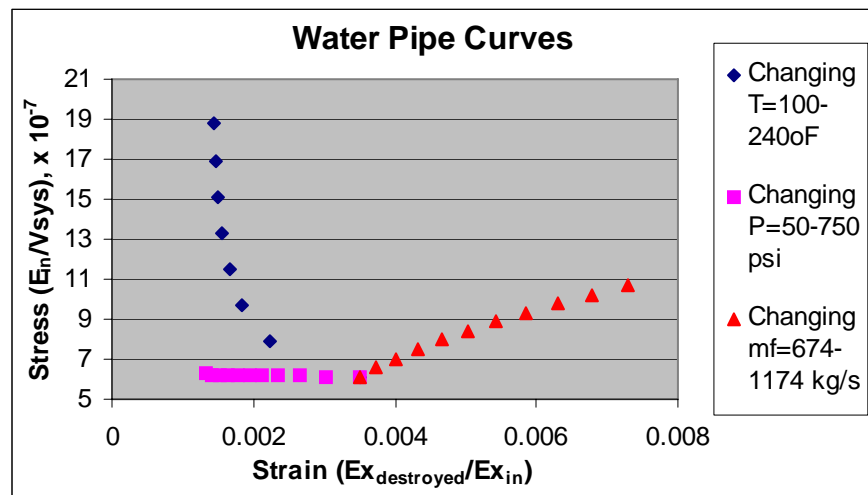
Figure 22: Water Pipe Results (as part of the Overall System Simulation)

Results from the simulation of the water pump from the overall system layout are shown below in Figure 23. The observed temperature trend is equivalent to the trend determined by hand calculations in Figure 11 – an inverse relationship between stress and strain. While the changing pressure case was not investigated as an individual case, the behavior exhibited during the simulation when changing the pump's inlet water

pressure can be observed to be equivalent to the behavior observed on the composite pump graph in Figure 17 – an inverse relationship between stress and strain covering a narrow stress range. The changing flow rate behavior differs for the simulation as compared to the curve shown in Figure 12. However, there are significant differences between the hand calculation case and the simulation settings. First, the volumetric flow rate was changed for the hand calculations versus the mass flow rate changed for the simulation. While the hand calculations resulted in a direct relationship, the stress range covered was extremely small (approximately stress = 10^5). The inverse relationship for the simulation covers a large stress range (on the order of $4\text{x}10^{10}$). The simulation pump was assumed to operate on a constant delta pressure basis – no matter the flow rate, the efficiency and delta P imparted by the pump remained constant. The hand calculation pump assumed a relationship between efficiency, volumetric flow rate, and head. Thus, as the flow rate increased, the pump head also increased allowing the additional energy imparted by the extra flow to be balanced with additional exergy destruction. No such balance is present in the simulated pump.
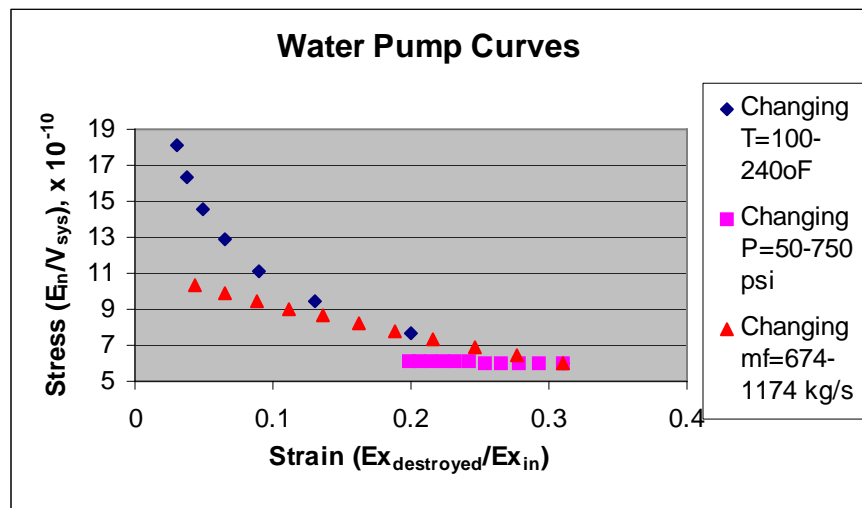

Figure 23: Water Pump Results (as part of the Overall System Simulation)

Results from the final piece of equipment simulated, the heat exchanger, are shown in Figure 24. There are some significant differences between the simulated behavior and the hand-calculated behavior from Figures 13 and 14. The original hand calculations only varied the inlet water temperature and inlet steam mass flow rate, so only those trends will be compared. The changing inlet water temperature trend from Figure 14 displayed a direct relationship reaching a maximum stress value before changing to an inverse relationship between stress and strain. The curve in Figure 24 shows a direct relationship reaching a minimum strain value before changing to an inverse relationship. However, there are significant differences between the systems used – the hand calculation system allowed the exchanger length to vary such that the outlet steam stream was completely condensed for each change – in the simulator case the length was constant and the steam outlet stream was not able to completely condense for the data points related by the inverse relationship. Since the volume is fixed, as the inlet temperature increases, the inlet stress will increase. However, since the excess capacity of the exchanger is decreasing, less heat is being exchanging, thus destroying proportionally less exergy and allowing the strain value to decrease. The opposite is true for the hand calculation case where the length increases – while the stress value is again increasing due to the energy into the exchanger from the higher inlet temperature increasing faster than the volume, the added volume allows the exchanger to have more capacity to exchange heat, thus more exergy is destroyed by heat exchange. For the changing steam mass flow rate curve, the inverse simulated relationship is again different from the direct hand-calculated relationship. The reasons for this difference are again due to the differences in exchanger geometry for the two cases.
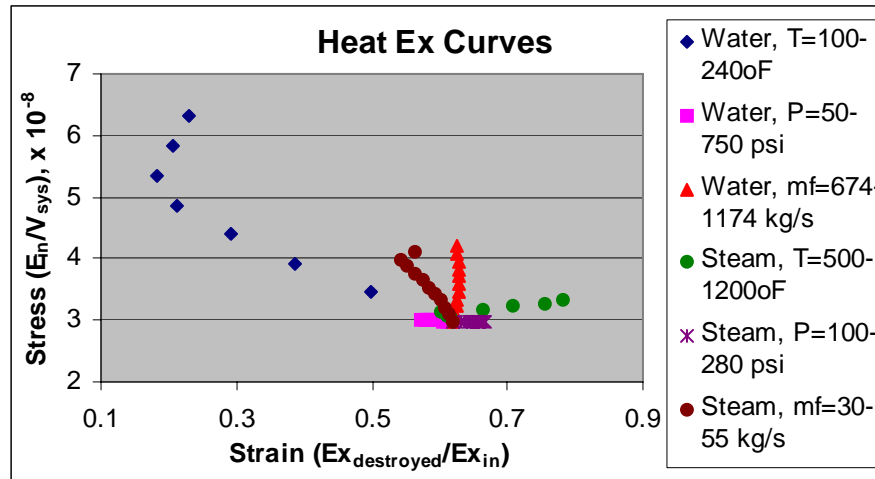
Figure 24: Heat Exchanger Results (as part of the Overall System Simulation)

Combined System Results

The use of the process simulator allowed equipment to be easily combined by linking outlet and inlet streams. Thus, the methodology's ability to capture individual equipment limitations in overall system results could be determined. The overall system curve for the combined water pipe, water pump, steam pipe, and heat exchanger system was created by taking the system inputs as the material streams into the water pipe and steam pipe and the energy stream into the pump while the output streams were the tube and shell side streams from the exchanger. The graph is shown below in Figure 25.

Figure 25: Overall System Curves from Process Simulation

Like the individual system graphs, all the curves begin at a common stress and strain point. The data for this overall system look most like the data from the heat exchanger case. The changing water temperature trend is again an inverse relationship as it was for the water pipe, pump, and heat exchanger curves. While the overall system curve reaches a minimum strain value like the heat exchanger curve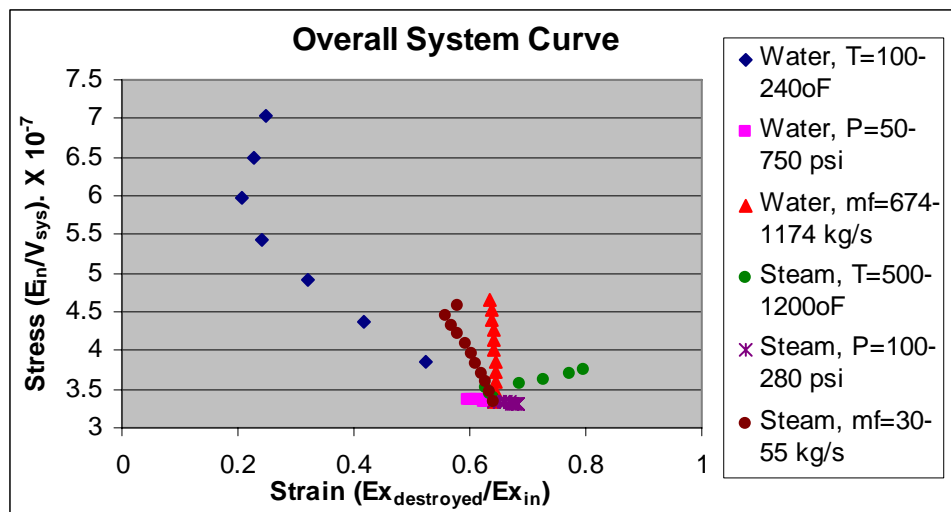, this minimum value is higher (strain approximately 0.2) than the value from the heat exchanger case (strain approximately 0.18). The additional pieces of equipment cause the stress values to decrease (mostly due to the presence of a larger system volume). The changing water pressure case displays the inverse relationship observed for the water pipe, water pump, and heat exchanger: again, the stress range covered is small due to little change in the energy load with increasing pressure. The changing water mass flow rate was observed to result in different trends for different equipment: a direct relationship for the water pipe, an inverse relationship for the water pump, and a direct relationship covering a very small strain range for the heat exchanger. The overall system has a very slightly inverse relationship between stress and strain for the changing water mass flow rate. The reason the water pump relationship is conserved is due to the strain ranges and order of magnitude of the individual unit data. The water pump curve covers a relatively large

strain range (strain from 0.05391 to 0.3096) as compared to the range for the heat exchanger (strain from 0.6202 to 0.6261) or the water pipe (0.003498 to 0.007303). This large range coupled with the large stress values for water pump (stresses on order of 10^{11} for the pump versus 10^8 for the exchanger) resulted in the overall data shifting to a slight inverse relationship with a small strain range (strain from 0.6417 to 0.6836). The influence of the heat exchanger can be observed in both the high strain values and the small range. The water pipe data influence is negligible for the overall system due to the relative order of magnitude of the data: the pipe strain values are 10 to 100 times smaller than the ranges for the pump or heat exchanger because the pipe operates extremely close to ideality.

The changing steam temperature curve displays a direct stress-strain relationship similar to the relationship from the steam pipe and heat exchanger curves. The strain range (strain from 0.6417 to 0.7976) is remarkably close to the range from the heat exchanger case (0.6202 to 0.7829) with the decrease partially attributable to the added effect of the steam pipe (original strain range of 0.01653 to 0.04302). The inverse stress-strain trend observed for the steam pipe and heat exchanger changing steam mass flow rate curve is also observed in the overall system. The minimum strain behavior of the curve from the heat exchanger is again observed in the overall system when the exchanger fails to condense all the steam present. The changing steam pressure curve trends differ from the steam pipe (weak direct relationship) and the heat exchanger (weak inverse relationship), however the overall system displays a weak inverse relationship. One reason for the conservation of the inverse relationship seen with the heat exchanger is the magnitude of the strain values: the steam pipe strain values range from 0.01456 to 0.01653 while the heat exchanger values range from 0.6202 to 0.6666. The heat exchanger strain values are both larger and vary over a large range, thus their behavior dominates the overall trend.

Range Comparison

Another test for the combined system was ensuring the ranges predicted by the quantification method for the overall system were smaller than or equal to the ranges dictated by the individual equipment data. Since the overall system contained the individual equipment, it range was limited by constrains of the most restrictive individual equipment range. The data ranges were determined using the same methodology described in the "Quantification" chapter by performing power-law regression on each of the stress-strain data series and determining where the trend-line R^2 value dropped below 0.99. The data comparing each of the four individual equipment ranges with the overall system range are shown below in Table 17.

Table 17: Allowable Range Comparison for Overall Simulated System

Curve #	Initial Value	Maximum Allowable Value				
		Wpipe	**Wpump**	**Spipe**	**HeatEx**	**Overall**
1	W T=100°F	140°F	all ok	n/c	220°F	200°F
2	W P=50 psi	500 psi	all ok	n/c	all ok	all ok
3	W m$_f$=674 kg/s	all ok	1074 kg/s	n/c	824 kg/s	774 kg/s
4	S T=500°F	n/c	n/c	900°F	900°F	900°F
5	S P=100 psi	n/c	n/c	200 psi	180 psi	180 psi
6	S m$_f$=30 kg/s	n/c	n/c	all ok	45 kg/s	47.5 kg/s

The notation "n/c" on the table indicates the equipment parameters did not change for that specific variable change: for example, a change affecting the steam stream would have no effect on the water pipe or pump. The notation "all ok" indicates the R^2 value did not drop below 0.99 for the entire variable range. The results show that the overall range is lower or equal to the range predicted for each of the individual pieces of equipment with a few notable exceptions. The main exception is the water pipe, both for the changing pressure and changing temperature cases.

The main reason the water pipe ranges are not captured in the overall system range is due to the differences in order of magnitude – the water pipe operates at strain rates 10 to 100 times less than the strain values from other pieces of equipment. The water pipe operates extremely close to ideality – little exergy is lost due to friction and even less due to heat transfer to the environment. Thus, even if the exergy destroyed within the pipe doubles, the strain values are still many times smaller than other units and when summed as part of the overall system, the effects of even large percentage changes within the water pipe are still negligible.

The other exception is the heat exchanger range for the changing inlet steam mass flow rate: the range predicted for the heat exchanger is one increment smaller than the range predicted for the overall system. The R^2 value for heat exchanger falls from 0.9922 to 0.9891 as the mass flow rate increases from 45 to 47.5 kg/s while the overall system R^2 value falls from 0.9919 to 0.9889 as the mass flow rate increases from 47.5 to 50 kg/s. The discrepancies with these ranges could be due to rounding in calculations, assumptions within the simulation, or choice of increment.

The overall ranges as compared with the individual equipment ranges show promise in being able to predict individual equipment limitations within an overall composite system. This is imperative in showing the proposed resilience quantification method can be used to find safe operating ranges.

METHODOLOGY DISCUSSION

While the original test systems as well as the simulations included equipment and process limitations, because of the simplicity of test systems and assumptions associated with the simulation, some aspects of the system's response to detailed limitations may not have been present. For example, properties of the pipe such as additional vibrations that may have occurred at higher mass flow rates were not included. While the simulation likely included more accurate details than the hand calculations, the simulation certainly did not include detailed metallurgical limitations and other related parameters which would be required to determine specific failure points. Other

limitations such as required partial pressures for reaction or minimum concentrations for sensor detection were also not included due in part to the lack of an associated control system for the simulated system and the lack of a reaction within the system. Possible approaches for future use of this methodology in light of these limitations include not allowing extremely critical parameters to vary (vary other system parameters) or ensuring the system's energetic response is detailed enough to reflect departure from those conditions. An example of how the detail would be necessary is the case of a reaction that required a certain concentration. The system's energetic response (as shown on a characteristic system response curve) would change if no reaction occurred (the base case would be set to where the reaction was occurring). This change would likely cause the allowable range to end due to deviations from the stress-strain trend established for the system when the reaction was occurring.

Another point of discussion is the accuracy of the predicted ranges. The range may be limited due to fluid properties changes or due to equipment limitations. For example, the allowable pipe operating range is likely limited due to fluid property limitations as the limits seem far from any known failure points (maximum operating temperature and pressure of a steel pipe, etc). If the range ends due to fluid property limitations, an action like increasing the pipe's design pressure will have no effect. However, if the range limits are due to equipment limitations, changes to equipment specifications will cause changes in the energy behavior of the system as it approaches those limitations and thus an action like increasing the design pressure of the pipe will increase the allowable range. For example, if the pipe range were limited by equipment limitations, raising the design pressure would cause the pipe to cease to dissipate energy through modes such as material deformation.

Physical properties of the process fluids (density, internal energy, etc) many not show predictable or consistent behavior, thus these property changes may be sufficient to cause the energetic performance of the system to deviate from the power-law trend. This is especially concerning for fluids like water that display atypical behavior for different conditions. While deviations caused by fluid properties will likely not cause catastrophic

failure (like equipment failures may), these limitations may cause the system to be more difficult to control and operate. These properties also complicate abilities to understand system behavior and interactions. The different type of system deviations (equipment versus fluid) that cause the power-law trend to end can be viewed as examples of the resilience aspects of strength and flexibility. The strength aspect of resilience can be seen within by equipment limitations while the fluid properties contribute in part to the system's flexibility. While these properties are manifested differently in systems and consequences of overstepping their bounds differ, both contribute to resilience and must thus be considered when understanding system behavior.

Finally, while departure from a power-law trend has been used to signify changing system behavior for this research, it is possible that for certain systems this may not be sufficient or appropriate. The system may display another functional relationship or system properties may not allow prediction of system properties at all. However, the ability to have one, unified method for determining appropriate ranges makes the power-law method very attractive. As with any other methodology, it is possible that the ranges predicted from power-law analysis may be more accurate (and appropriate) for certain applications. For example, the pump ranges predicted resilient operation to end approximately 10 to 20$^\mathrm{o}$F from a known failure point, the onset of pump cavitation. On the contrary, the water pipe ranges cut-off well before any known pipe failure points. While these ranges are most likely due to fluid property variations, the predicted ranges seem overly conservative. While the inclusion of more detailed process parameters and limitations may improve the accuracy of predicted limits, it is certainly more desirable that ranges be overly conservative rather than the opposite.

METHODOLOGY STRENGTHS AND WEAKNESSES

While the resilience method developed shows promise, the results presented have included some notable weaknesses that provide opportunities for future improvement. The sensitivity of the method to individual units within an overall system is not as robust as would be desired – this was demonstrated with the results for the water pipe within

the overall simulation. Since the overall graphs and results in effect sum the behavior of individual systems, perhaps weighing factors for important units could be introduced to ensure the methodology appropriately includes important limiting factors.

The effect of noise has not be assessed – since the methodology relies on the accuracy of the data to obtain an accurate R^2 value, it is not known if the presence of noise would introduce enough scatter to invalidate that approach. Also, the methodology relies on definitively determined boundaries for analysis. The test systems only included a few material and energy streams, but actual systems have numerous streams. It may be difficult to determine the behavior of all included streams for all variable changes. If stream properties cannot be calculated, stress and strain variables cannot be determined. Finally, the methodology cannot be applied to non-physical system components – the energy changes caused by human decisions or economic factors within systems would be included, but the actual decision and its associated justifications or thought processes would not be represented.

Some strengths of the methodology not already touched on include its flexibility of reference states – since the exergy reference temperature and pressure can be set to ambient conditions, the reference state can be set to different values for processes in warm or cold climates. For example, different results for different seasons could be obtained by changing the reference temperature. The use of a general "energy in" allows the methodology to be applied to a variety of different systems without having to translate a great deal of discipline-specific terminology or principles.

SUMMARY

Each of the individual systems analyzed with hand calculations (water pipe, water pump, steam pipe, and heat exchanger) were combined into an overall system using the ASPEN process simulator. Trends from the simulated individual equipment results were compared with the individual unit results as well as with the overall system results.

The ranges predicted for the overall simulated system were compared with the ranges for each of the simulated system components. With a few exceptions, the computation of an overall range allows individual equipment limitations to be captured and combined into a singular range. The agreement of these ranges indicates the scalability of the method. Some remaining questions resulting from the application of the resilience concept to an overall system were summarized as well as the strengths and weaknesses of the current methodology.

CHAPTER VIII
FUTURE WORK AND CONCLUSION

While encouraging results have been presented as to the validity and applicability of the proposed system resilience concept and associated methodologies, significant questions remain. Many opportunities exist both to strengthen the methodology as well as for its expansion.

FUTURE OPPORTUNITIES

While basic applications and system types were explored by this research, opportunities exist to determine if the system resilience concept could have wider application beyond the examples previously shown.

Integrate with Sustainable Approaches

This is a promising area touched on earlier in the "Framework of Existing Resilience Research" chapter. Exergy is often used in sustainability applications to gauge the environmental footprint or green effect of a certain process. The destruction of exergy is undesirable due to its limited nature – additional energy sources are required to perform future work if exergy is destroyed.

This research views exergy from a different perspective, however if exergetic properties of process stream could be calculated once and then applied (albeit in different ways) for both safety and environmental applications, both time and monetary resources could be saved. Also, by studying the similarities between the uses of exergy, it may be possible to find system designs which optimize both environmental and safety performance.

Compare with Optimization Methods

While the proposed methodology did not include any type of optimization, opportunities exist for comparison of results with those from existing optimization

methodologies. Optimal designs could be determined by finding designs that allow the largest resilient operating ranges.

For example, if the diameter of a pipe is being optimized from an economic perspective, the cost of energy lost due to heat loss to the atmosphere and friction must be balanced against the increased cost of larger pipes. An optimal diameter can be determined by combining energy and maintenance costs with annualized capital costs and finding the diameter that minimizes the total cost. The economic optimal diameter could be compared with the diameter that maximizes the resilient range for different variables. This is also one way in which economic considerations could be factored into the resilience methodology.

Add Other Exergy Destruction Modes and Energy Sources

The examples used for the development of the concept included two exergy destruction modes: friction and heat transfer across a finite temperature difference. System complexity could be increased by adding other exergy destruction modes such as mixing or chemical reaction.

The examples used in this work included two sources of energy: energy of material streams and electricity into the pump. Other energy sources such as potential energy from elevation changes as well as kinetic energy changes from significant velocity differences could be introduced to determine their affect on processes.

Use Other Process Fluids

All the examples provided used water as the process fluid due to the availability of water properties. However, the inclusion of other process fluids would allow the effect of equipment versus material behavior to be more easily viewed. For example, if the same system (same equipment dimensions, same parameters such as flow rate, temperature, and pressure) containing a different process fluid were analyzed, would the results differ? The degree to which the results differed would be evidence to how much effect the material versus equipment limitations has on the process' resilience.

While the availability of material properties was an issue in the nascent stages of this research when calculations were performed using Excel, it is less of a concern when using the process simulators. The process simulator will calculate the thermodynamic properties of a variety of different materials, thus making the inclusion of other materials a challenge only from the perspective of defining the exergetic reference state for any composition changes.

Integrate with Process Control Analysis

Both this resilience concept and process control analysis determines ranges for process operation. The limitations of many systems are determined by the limitations of the control system used to regulate process conditions. Control systems rely on the use of appropriate models of system performance to predict the effect of variable changes on the desired inputs and outputs. While measurement comparisons help to correct any discrepancies between measured and predicted variables, the stability of the response becomes an issue.[58] Thus, the models used to predict system behavior are often only useful for certain variable ranges. The addition of control system limitations may make the resilient ranges more informative as well as vise versa: the resilient ranges may provide important information about process regions were behavior is similar enough to be accurately predicted by a process model.

Apply to Real Process Data

This methodology relies on accurate data to determine functional relationships between system stress and strain. All examples presented have been idealized in one important manner – there was no noise present in the measured variables. If data from a real-life unit or process were used, there would be scatter present due to sensor noise, natural fluctuation of utility parameters, and variation in the properties of other process streams. The properties within a unit would also vary depending on where parameter measurements were taken (such as near wall/near center of vessel or in the vicinity of flow obstacles). It is unknown whether the presence of scatter would render the use of

the R^2 value untenable. While it might be possible to smooth out some of the scatter or noise, its presence might decrease the correlation of determination to the level that the resilient range cut-offs would have to be adjusted.

Addition of More Equipment Limitations

Another area for expansion is the addition of more detail equipment parameters. While equipment limitations such as the pump's decrease in efficiency as the flow rate changed were included, more detailed degradation of equipment behavior was not included mainly due to limitations of available information. For example, the pump may begin to dissipate energy by vibration or additional noise as the flow rate increases – this energy loss was not included in the previous analysis. For the pipe, as the pressure and temperature increase, the pipe may vibrate or the metal may deform slightly.

The addition of more detailed equipment limitations will aid in predicting more accurately safe operating ranges as well as providing valuable information about how ranges change when equipment types and specifications are altered.

CONCLUSION AND SUMMARY

The background and development of the concept of resilience for physical, engineered systems has been presented. This concept was explored with the objective of better protecting modern systems from the myriad of possible failures to which they are susceptible, as well as providing more information about the effects of different parameters on the stability and operability of these systems. To help achieve this objective, the research goals were set as defining the concept of system resilience, determining how systems would manifest resilience, developing quantitative correlations to assess and compare resilience, and finally determining how this concept can be integrated into the design process. The resilience concept was explored due to its incorporation of desired characteristics of strength, or robustness, and flexibility.

Background and Development of Concept

Background research related to the resilience concept was presented, including self-healing plastics, self-healing computer systems, resilient naval ships, and resilient power grids. Related research terms such as redundant, scalable, self-managing, robust, and decentralized were defined in order to explore some desired system characteristics. The manner in which the resilience concept has been used in ecology, psychology, information science, as well as materials science was explained.

Resilience as viewed within complex systems analysis was explained. System aspect classifications including physical, informational, financial, and behavioral were explained as well as the relation of resilience to sustainability. These topics and classifications were explored to help focus this research's scope. It was determined that this research would be limited to physical systems and that physical system resilience would be developed as a quantifiable, inherent property of systems. The materials science definition for resilience was used as an inspiration for this research's definition. Thus, resilience was defined as the amount of energy a system can store without failure or instability.[19]

General Framework for Visualization

System energy, irreversibility, and exergy were defined and discussed and the relationship between energy and safety was explored. These concepts were used to define system stress and system strain variables to allow system resilience to be visualized using a characteristic system response curve similar to how a stress-strain curve is used to visualize material resilience. System stress was defined as the energy input into a system divided that system's volume while system strain was defined as a ratio of the system's exergy, or potential to do work on itself or its surroundings.

Demonstration for Smaller Units

In order to create characteristic system response curves, simple test systems including a steam pipe, a water pipe, a water pump, and a heat exchanger were

"stressed" by applying series of variable changes. Properties of the test systems were explained and performed calculations were detailed. Inlet conditions for each test case were fixed with energy and exergy balances conducted for each test system to determine outlet stream conditions. Stress and strain variables were calculated first for the base case and then again as process parameters such as mass flow rate, temperature, and pressure were increased incrementally.

Results were presented in the form of characteristic system response curves for each variable changed (flow rate, temperature, and pressure) for each test case. The significance and trends of these curves were discussed. The individual stress curves for each test system were shown in combination on composite system response curves for each of the test systems along with changing variable curves for starting conditions other than the original base cases.

Method of Range Determination

To determine which regions of the characteristic response curves displayed resilient behavior, a method for quantitatively determining resilience was proposed. A power-law trend was used to predict the stress-strain behavior for each characteristic system response curve, with departure from resilience characterized by a drop in the regression coefficient of determination. This methodology allowed the resilient range to vary for different systems, different stresses to the same system, as well as different initial conditions for the same system. Resilient ranges were determined for each test case and variable change with range behavior with changing process variables discussed and compared.

Simulation of Overall System and Comparison of Results

All four test systems were combined into an overall system whose behavior was simulated using the process simulator ASPEN. Trends for the individual equipment graphs constructed from simulated data were described and those trends compared with results from hand calculations. Characteristic system response curves for the overall

system were also graphed and these trends compared with those observed for the individual equipment curves.

Resilient ranges were determined for both the individual equipment and the overall system by performing power-law regression. The overall ranges were compared with the individual equipment ranges – for the method to demonstrate proper scalability, the ranges obtained for the overall system would need to be smaller than or equal to the ranges calculated for each individual piece of equipment. With the exception of the water pipe, the overall ranges did reasonably well at capturing the limiting behavior of the individual equipment in the overall, combined range.

Methodology Discussion, Strengths and Weaknesses

A discussion of some important issues and questions concerning the methodology was provided. The lack of detailed system limitations for the given test examples was discussed as well as examples given of how more detail could provide more accurate allowable ranges. The accuracy of the predicted ranges was addressed along with how fluid limitations versus equipment limitations might be manifested in the predicted allowable ranges. Finally, conservatism that may be present in the predicted ranges was discussed.

Strengths and weaknesses of the methodology were discussed along with a few possible remedies. Weaknesses such as possible noise effects, challenges related to the combination of systems with different scale stress and strain variables, difficulties of determining all stream properties for actual process systems, as well as the limitations of applying the methodology only to physical system aspects were discussed. Strengths mentioned included the ability to change reference conditions as well as the near-universality of energy for easy application of the methodology to other physical systems.

Outlining of Future Opportunities

Finally, future opportunities for expansion of this work were presented. It is recognized that despite the work presented, this research is still in its nascent stages and

while many promising results have been presented, there are many question still unanswered, many weaknesses which must be investigated, and applications which must been explored. Other examples that could be used to support the methodology and further explore its strengths and weaknesses include the use of other process fluids (besides water), the addition of other input energy sources, the inclusion of additional exergy destruction modes, inclusion of more detailed process limitations, and the application of the method to real process data to explore the effect of noise on the methodology. Some possible arenas for expansion of this methodology include integration with sustainability research, exploration of possible links with process control, and comparison of results with those from optimization methods.

REFERENCES

1. Parker, D. (1937). *Explosion in School Building at New London, Tex., March 18, 1937, Report of Investigations*. Washington, DC: U.S. Bureau of Mines.

2. Bogard, W. (1989). *The Bhopal Tragedy — Language, Logic and Politics in the Production of a Hazard*. Boulder, CO: Westview Press.

3. The National Commission on Terrorist Attacks Upon the United States. (2004). *The 9/11 Commission Report*. New York: W. W. Norton, & Co. Available at http://www.9-11commission.gov/report/index.htm.

4. Mish, F. (Ed.). (2006). Resilience. *The Merriam-Webster Dictionary Online*. Available at http://www.m-w.com/cgi-bin/dictionary?book=Dictionary&va=resilience.

5. Picket, S., Cadenasso, M., & Grove, J. (2004). Resilient cities: Meaning, models, and metaphor for integrating the ecological, socio-economic, and planning realms. *Landscape and Urban Planning, 69*, 369-384.

6. Ludwig, J., Coughenour, M., Liedloff, A., & Dyer, R. (2001). Modeling the resilience of Australian savanna systems to grazing impacts. *Environmental International, 27*, 167-172.

7. Holling, C. (1996). Engineering resilience versus ecological resilience. In *Engineering within Ecological Constraints* (pp. 31-44). Washington, DC: National Academy Press.

8. Arrowsmith, C., & Inbakaran, R. (2002). Estimating environmental resiliency for the Grampians National Park, Victoria, Australia: a quantitative approach. *Tourism Management, 23*, 295-309.

9. Alo, R., de Korvin, A., & Modave, F.(2003). Decision Making for Robust Resilient Systems. In *Proceedings of the 36th Hawaii International Conference on System Sciences*. Available at http://csdl2.computer.org/comp/proceedings/hicss/2003/1874/02/187420057c.pdf.

10. Li, Y., Rao, F., Chen, Y., Liu, D., & Li, Y. (2004). Services Ecosystem: Towards a Resilient Infrastructure for On Demand Services Provisioning in Grid. In *Proceedings of the IEEE International Conference on Web Services*. Available at ieeexplore.ieee.org/iel5/9185/29136/01314763.pdf.

11. Huang, C., Peng, H., & Yuan, F. (2005). A Deterministic Bound for the Access Delay of Resilient Packet Rings. *IEEE Communications Letters*, *9*, 87-89.

12. Coutu, D. How resilience works. *Harvard Business Review, 80*, 46-52.

13. Barbanel, L. (2002). Fostering resilience in response to terrorism: A fact sheet for psychologists working with adults. *APA Task Force on Resilience in Response to Terrorism.* Available at http://www.apa.org/psychologists/pdfs/adults.pdf.

14. Hamel, G., & Valikangas, L. (2003). The quest for resilience. *Harvard Buisness Review*, *81*, 52-63.

15. Key-to-Steel. (Accessed 2006). Resilience. *Knowledge Article.* Available at http://www.key-to-steel.com/Articles/Art41.htm.

16. Considine, D. (Ed.). (1983). Resilience. In *Van Nostrand's Scientific Encyclopedia,* 6th ed. New York: Van Nostrand Reinhold Company.

17. Kuisma, R., Redsven, I., Pesonen-Leinonen, A., Sjoberg, A., & Hautala, M. (2005). A practical testing procedure for durability studies of resilient floor coverings. *Wear*, *258*, 826-834.

18. Bouvet, P., & Vincent, N. (2000). Optimization of resilient wheels for rolling noise control. *Journal of Sound and Vibration, 233*, 765-777.

19. Mitchell, S., & Mannan, M. (2006). Designing resilient engineered systems. *Chemical Engineering Progress, 104*, 39-45.

20. White, S., Sottos, N., Geubelle, P., Moore, J., Kessler, M., Sriram, S., Brown, E., & Viswanathan, V. (2001). Autonomic healing of polymer composites. *Nature*, *409*, 794–797.

21. Chen, X., Dam, M., Ono, K., Mal, A., Shen, H., Nutt, S., Sheran, K., & Wudl, F. (2002). A thermally re-mendable cross-linked polymeric material. *Science*, *295*, 1698-1702.

22. Slowik, M. (2004). Research: Self-Healing Materials Using Electrohydrodynamics. Available at www.princeton.edu/~cml/html/research/self_healing.html.

23. Lee, J., Buxton, G., & Balazs, A. (2004). Using nanoparticles to create self-healing composites. *Journal of Chemical Physics*, *121*, 5531–5540.

24. Koopman, P. (2003). Elements of the Self-Healing System Problem Space. In *Workshop on Architecting Dependable Systems (WADS03)*. Available at www.ece.cmu.edu/~koopman/roses/wads03/wads03.pdf.

25. George, S., Evans, D., & Marchette, S. (2003). A Biological Programming Model for Self-Healing. In *First ACM Workshop on Survivable and Self-Regenerative Systems (SSRS03)*. Available at www.cs.virginia.edu/~evans/pubs/ssrs.pdf.

26. Goel, S., Belardo, S., & Iwan, L. (2004). A Resilient Network that Can Operate Under Duress: To Support Communication between Government Agencies during Crisis Situations. In *Proceedings of the 37th Hawaii International Conference on System Sciences*. Available at http://csdl2.computer.org/comp/proceedings/hicss/2004/2056/05/205650123a.pdf.

27. Gruber, C. (2003). Resilient Networks with Non-Simple p-Cycles. In *Proceedings of the 10th International Conference On Telecommunications*. Available at http://www.lkn.ei.tum.de/~claus/publications/Gruber2003ResilientNetworksNon SimplePCycles.pdf.

28. Mish, F. (Ed.). (2006). Robust. *The Merriam-Webster Dictionary Online*. Available at http://www.m-w.com/cgi-bin/dictionary?book=Dictionary&va=robust.

29. Carlson, J., & Doyle, J. (2002). Complexity and robustness. In *Proceedings of the National Academy of Sciences of the United States of America, 99,* 2538-2545.

30. Venere, E. (2001). Engineers Will Demonstrate New System to Prevent Power Failures. *Science Daily.* Available at http://www.sciencedaily.com/releases/2001/03/010305071849.htm.

31. Venere, E. (2000). Future U.S. Warships Will be Automated. *Purdue News.* Available at http://news.uns.purdue.edu/html4ever/000107.Sudhoff.futureships.html.

32. Morari, M. (1983). Flexibility and resiliency of process systems. *Computers & Chemical Engineering*, *7*, 423–437.

33. Ohno, H., & Nakanishi, E. (1985). Dynamic resiliency of heat-integrated distillation systems. *Institute of Chemical Engineers Symposium Series, 92(Process Syst. Eng.),* 469–479.

34. Fiksel, J. (2003). Designing resilient, sustainable systems. *Environmental Science Technology*, *37*, 5330-5339.

35. Fiksel, J. (2006). Sustainability and resilience: Toward a systems approach. *Sustainability: Science, Practice, & Policy, 2*, 14-21.

36. Kletz, T. (1998). *Process Plants: A Handbook for Inherently Safer Design*. Philadelphia: Taylor & Francis.

37. Fuchs, H. (1996). *The Dynamics of Heat*. New York: Springer.

38. Szargut, J. (1980). International progress in second law analysis. *Energy*, *5*, 709-718.

39. Microsoft. (1999). Clip Art Gallery. *Microsoft Word*. Redmond, WA: Microsoft Corporation.

40. Szargut, J., Morris, D., & Steward, F. (1988). *Exergy Analysis of Thermal Chemical and Metallurgical Processes*. New York: Hemisphere Publishing.

41. Wikipedia contributors. (2007). Exergy. In *Wikipedia, The Free Encyclopedia*. Available at http://en.wikipedia.org/w/index.php?title=Exergy&oldid=87473265.

42. Wikipedia contributors. (2007). Stress (physics). *Wikipedia, The Free Encyclopedia*. Available at http://en.wikipedia.org/w/index.php?title=Stress_%28physics%29 &oldid=8898792445.

43. Atkins, P. (1998). *Physical Chemistry,* 6th ed. New York: W. H. Freeman and Company.

44. Smith, J., Van Ness, H., & Abott, M. (2001). *Introduction to Chemical Engineering Thermodynamics,* 6th ed. New York: McGraw-Hill Higher Eduction.

45. Nelik, L. (1999). *Centrifugal and Rotary Pumps – Fundamentals With Applications*. New York: CRC Press.

46. Seider, W., Seader, J., & Lewin, D. (1999). *Process Design Principles: Synthesis, Analysis, and Evaluation.* New York: John Wiley & Sons.

47. Engineers Edge. (2007). Properties of Metals – Thermal. *Material Specifications and Characteristics – Ferrous and Non-Ferrous.* Available at http://www.engineersedge.com/properties_of_metals.htm.

48. Spang, B. (2002). Water97_v13.xla – Excel Add-In for Properties of Water and Steam in SI-Units. Available at http://www.cheresources.com/iapwsif97.shtml.

49. Menon, E. (2005). *Piping Calculations Manual*. New York: McGraw-Hill.

50. Darby, R. (2001). *Chemical Engineering Fluid Mechanics,* 2nd ed. New York: Marcel Dekker, Inc.

51. Incropera, F., & DeWitt, D. (1996). *Introduction to Heat Transfer,* 3rd ed. New York: John Wiley & Sons.

52. Otero, L., Molina-García, A., & Sanz, P. (2002). Some interrelated thermophysical properties of liquid water and ice. I. A user-friendly modeling review for food high-pressure processing. *Critical Reviews in Food Science and Nutrition, 42*, 339–352.

53. Hewitt, G. (1992) Condensers. In *Handbook of Heat Exchanger Design.* New York: Begell House, Inc.

54. Gedeon, M. (2001). Elastic Resistance. *Technical Tidbits, 3*, 1-2. Available at http://www.brushwellman.com/alloy/tech_lit/april01.pdf.

55. Carlson, J., & Doyle, J. (1999). Highly optimized tolerance: A mechanism for power laws in designing systems. *Physical Review E*, *60*, 1412-1427.

56. Barnes, H. (1999). The yield stress – a review or 'παντα ρει' – everything flows?. *Journal of Non-Newtonian Fluid Mechanics*. *81*, 133-178.

57. Sincich, J., Levine, D., & Stephan, D. (2002). *Practical Statistics by Examples Using Microsoft Excel*[®] *and Minitab*[®]*,* 2nd ed. Upper Saddle River, NJ: Prentice Hall.

58. Dorf, R., & Bishop, R. (1995). *Modern Control Systems*, 7th ed. Reading, MA: Addison-Wesley Publishing Company.

VITA

Susan McAlpin Mitchell received her Bachelor of Science degree in chemical engineering in May 2003 from Texas A&M University. She entered the PhD program in chemical engineering at Texas A&M University in August 2003 and soon began research focused on chemical engineering process safety with the May Kay O'Connor Process Safety Center.

Ms. Mitchell has completed summer internships with the National Park Service, Celanese Chemicals, the United States Naval Research Laboratory, Sandia National Laboratory, and ExxonMobil Chemicals. Her post-graduation plans include taking a job with ExxonMobil Chemicals. Her publications include "Resilient Engineered Systems" with M. Sam Mannan in *Chemical Engineering Progress* (April 2006) and she has presented her research at conferences including the 2006 Mary Kay O'Connor Process Safety Symposium, the First International Conference on Self Healing Materials, and the 9th Process Plant Safety Symposium.

Ms. Mitchell can be reached via the Mary Kay O'Connor Process Safety Center, The Texas A&M University System, 3122 TAMU, College Station, TX 77843-3122. Her e-mail address is smmitchen@gmail.com.